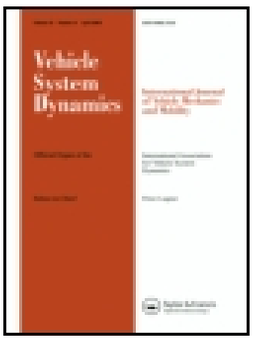

Vehicle System Dynamics

ISSN: 0042-3114 (Print) 1744-5159 (Online) Journal homepage: http://www.tandfonline.com/loi/nvsd20

Cross-wind effects on road and rail vehicles

Chris Baker , Federico Cheli , Alexander Orellano , Nicolas Paradot , Carsten Proppe & Daniele Rocchi

To cite this article: Chris Baker , Federico Cheli , Alexander Orellano , Nicolas Paradot , Carsten Proppe & Daniele Rocchi (2009) Cross-wind effects on road and rail vehicles, Vehicle System Dynamics, 47:8, 983-1022, DOI: 10.1080/00423110903078794

To link to this article: https://doi.org/10.1080/00423110903078794

Vehicle System Dynamics
Vol. 47, No. 8, August 2009, 983–1022

Taylor & Francis
Taylor & Francis Group

Cross-wind effects on road and rail vehicles

Chris Baker[a]*, Federico Cheli[b], Alexander Orellano[c], Nicolas Paradot[d], Carsten Proppe[e] and Daniele Rocchi[b]

[a]School of Civil Engineering, University of Birmingham, Birmingham, UK; [b]Department of Mechanical Engineering Politecnico di Milano, Milan, Italy; [c]Center of Competence Aerodynamics & Thermodynamics, Bombardier Transportation, Hennigsdorf, Germany; [d]SNCF Rolling Stock Engineering Center, Le Mans, France; [e]Institut für Mechanik, Universität Karlsruhe, Karlsruhe, Germany

(*Received 28 May 2009; final version received 29 May 2009*)

This paper presents a review of recent research that has been carried out on the cross-wind effects on road and rail vehicles. After a brief introduction to the issues involved, the risk analysis framework is set out. All risk analysis methods require some knowledge of cross-wind aerodynamic force and moment coefficients, and methods of obtaining these through full scale and wind tunnel testing and through Computational Fluid Dynamics methods are then described. The picture of the flow fields around vehicles that is suggested by these measurements and calculations is then presented, and the steady and the unsteady aerodynamic force characteristics described. The detailed methodology for using this information to predict accident risk is then set out, including details of the vehicle dynamics system models that can be used. Finally potential alleviation methods are described and suggestions made for further works.

Keywords: railway accidents; road vehicle accidents; cross-wind effects; wind tunnel testing; computational fluid dynamics; risk analysis; vehicle dynamics

1. Introduction and background

The effects of cross-winds on road and rail vehicles can be broadly divided into two categories: effects due to high cross-winds and effects due to low cross-winds. In high cross-winds, road vehicles (and in particular high-sided lorries and vans) are blown over on a regular basis (see Figure 1).

An analysis of accident data in a major storm in 1991 [1] showed that accidents occurred when gust wind speeds were in excess of around 20 m/s, with the number of accidents occurring as the wind speed increased. Even if road vehicles are not blown over completely, cross-winds can result in course deviations that can themselves result in accidents [2]. The possibility of such accidents has led to the development of various mitigation schemes, usually based on meteorological warnings from either roadside anemometry or the local weather station, and

*Corresponding author. Email: c.j.baker@bham.ac.uk

ISSN 0042-3114 print/ISSN 1744-5159 online

DOI: 10.1080/00423110903078794
http://www.informaworld.com

Figure 1. An overturned lorry.

a staged series of vehicle restrictions as the predicted wind speed increases. Most long-span bridges around the world have such measures in place [3].

Another possible solution is to build wind fences on the side of the rail/road in the most sensitive parts of the line/motorway.

Trains are also at risk of blowing over in high cross-wind conditions and recent accidents have taken place in China [4], Japan [5], Belgium and Switzerland [6] (Figure 2). The wind speeds, necessary to blow trains over, tend to be rather higher than those for blowing road vehicles over – of the order of 35–40 m/s. Nonetheless these can occur in practice, and in the

Figure 2. Overturned trains.

design of any new trains these risks have to be taken very seriously indeed. This has led to the development of a number of standards [7] and [8] that address this issue and lay out rigorous risk-assessment procedures for new vehicles or for older vehicles that are required to operate on exposed routes. Such methods have been applied in Germany [9], France [10] and the UK [11]. In Italy, a similar approach is under study [12]. As well as the risk of a blow over accident, high cross-winds can affect trains in a number of other ways: excessive deflection between the overhead wire, and the pantograph and infringement of the kinematic envelope for example [13].

At rather lower wind speeds, the effects of cross-winds are not so pronounced but can still lead to operational difficulties: for example, Cooper has shown that there is a possibility of the excitation of suspension modes of high-speed trains in relatively low wind speed conditions [14], and road vehicle drivers can experience significant fatigue levels when driving in gusty winds.

This paper reviews the work that is being carried out into these effects. In Section 2, the risk analysis framework is set out. Sections 3 and 4 then consider the various experimental and computational techniques that are required to obtain vehicle aerodynamic information that can be used in the risk analysis. Section 5 describes, in rather general terms, the flow patterns that exist around road and rail vehicles in cross-winds, and Section 6 then goes on to consider both the steady and unsteady wind-induced forces and moments produced by these flow fields. Section 7 describes the interaction between these forces and the vehicle dynamic system, and Section 8 describes various risk-reduction methods. Finally in Section 9, some concluding remarks are proposed and recommendations for further work are made.

At this point it should be noted that this paper does not address a number of issues associated with wind effects on the transport infrastructure such as the disruptive effect of tree fall in high winds [15], the stability of road signs and signal gantries [16], the effect of cross-winds in enhancing the magnitude of lorry and train slipstreams [17] or the effect of cross-wind on vehicle passive ventilation systems [18]. These issues are of some significance in terms of safety and risk assessment, but are beyond the scope of the present paper.

2. The risk analysis context

2.1. *Safety policy and safety management*

Safety policy is specified by national governments or international agreements. Safety policies define the tolerability of risk up to concrete values. Safety management encompasses identification and analysis of specific risks and the prescription of safety criteria for risk assessment. In general, national authorities or operators are responsible for the safety management; operators are responsible for the risk analysis and manufacturers for the hazard analysis, although the level of regulation varies widely across countries and different transport sectors.

The collective risk (CR) [19] is defined by $R = \Sigma W_j A_j$. The sum extends over all identified hazards, W_j denotes the occurrence probability of a hazard in a certain amount of time or equivalent (for example, accidents per km for railway and road vehicles) and A_j its consequence, for example in terms of injuries, fatalities or costs due to damage. The CR could describe, for example, the expected number of fatalities per year. The individual risk (IR) is obtained from a similar expression, but with each term multiplied by with the probability of presence V_j of the individual when the hazard occurs: IR = $\Sigma V_j W_j A_j$.

From the collective and IR, tolerable hazard rates can be determined. Andersson *et al.* [6] proposes three methods to obtain hazard rates:

- ALARP: as low as reasonably practicable.

The cost involved in further reducing the CR should not be disproportionate to the benefit. This principle has its origin in the UK, see, for example, the legal finding [20].

- GAMAB: globalement au moins aussi bon.
  This French principle requires that a new system should have at most the same CR as a previously installed system.
- MEM: minimum endogenous mortality.
  This method, frequently applied in Germany, prescribes that the IR should be less than 10^{-5} per year. This number stems from the requirement that a new technique should not augment the minimum endogenous mortality, which is about 2×10^{-4} per year in industrial countries, by more than 5%.

Having defined a tolerable hazard rate, a risk matrix, containing the risk levels can be calibrated by classifying the hazard frequency and the consequences. Typical risk levels range from negligible, tolerable to unwanted and not tolerable. It is the task of the risk assessment to identify the risk level associated with a given incident scenario, for example for a specific vehicle and a specific timetable.

2.2. *Risk-assessment methods*

Assessing the risk of train overturning in a strong cross-wind is a complex procedure incorporating the occurrence probability for strong winds, the aerodynamic action of the wind on the train and vehicle dynamics. In some standards [21], risk assessment is circumvented by recurrence to reference vehicles which run safely in the past. However, such a procedure hinders innovation and does not allow the influence of preventive measures to be judged on an objective base. Therefore, various risk-assessment methods [14,22–24] have been proposed in the literature in order to quantify the risk of overturning for a specific vehicle on a specific track under strong cross-winds.

Cooper [14] proposed a risk-assessment procedure that is based on a quasi-static computation of a critical wind velocity for the vehicle: a reference wind velocity that is obtained from a 1 hour average wind velocity by application of various factors and a Gumbel distribution for the probability that the ratio of the wind speed and the reference velocity exceeds a critical value (the exceedance probability). The angle of attack of the wind is taken into account. Sensitivities in terms of changes of the overturning probability under parameter changes are stated.

Multiplication of the exceedance probability with the probability of the wind direction and integration over all possible directions yields then the overturning probability. The overturning probability per year, on the specific track segment, can be obtained by multiplying the former with the total exposure time of the vehicle during one year. The overturning probability for the whole line can then be computed by applying a series model for the individual segments of the track. A similar method is proposed in [24] for the risk assessment of the new Italian high-speed line.

Instead of the Gumbel distribution, a generalised extreme value distribution for extreme wind speeds has been proposed in [22], where also the effect of masking of gusts from different directions is discussed, when maxima are recorded. As a remedy, consideration of directional components of the wind speeds is proposed.

So far, the approach considered the extreme wind velocity as random, but all other components in the risk-assessment procedure were assumed to be deterministic. Carrarini [23] investigated the influence of uncertainties in the aerodynamic and vehicle dynamic part of the problem. To this end, an extreme value distribution is assumed for the 10-min average wind velocity at the site, but instead of a critical wind speed, a probability distribution for failure

as a function of the average wind speed is computed. This necessitates the introduction of a gust model and of random variables for the gust amplitude and duration as well as for the aerodynamic parameters.

All these assessment techniques require some knowledge of the aerodynamic forces and moments on vehicles. These are obtained either from full scale or wind tunnel tests or from Computational Fluid Dynamics (CFD) computations, and these methods are fully discussed in Sections 3 and 4.

2.3. *Risk analysis techniques*

The risk analysis lies in the centre of the risk-assessment procedure. Its objective is the determination of the probability of overturning under given boundary conditions. There are analytical methods based on extreme value statistics [25], semi-analytical methods [26] and numerical methods [27] available to carry out this task. All methods assume parametric models with random variables. Note that the random variables could also be obtained from a discretisation of stochastic processes or random fields. For cross-wind stability analysis, common random variables are wind gust parameters (amplitude and duration), if a gust model is adopted, aerodynamic coefficients and vehicle parameters such as mass and stiffness parameters. In order to keep the number of random variables small, sensitivity analysis methods are helpful to identify the most influential parameters of the problem and to provide important hints for efficient risk reduction methods.

2.3.1. *Analytical methods*

Analytical methods determine the failure probability of the vehicle system from an extreme value analysis. Frequently applied methods are the maximum and the peaks over threshold (POT) approach. For the maximum method, only n largest values of whatever parameter indicating system failure from n independent runs are taken and fitted to the Generalised Extreme Value distribution, whereas for the POT method all values above a certain, predefined threshold are taken and then fitted to the Generalised Pareto (GP) distribution. These distributions can subsequently be used to estimate the failure probability [25].

2.3.2. *Semi-analytical methods*

Semi-analytical methods can handle problems with a relative low number of random variables efficiently. They require a transformation of all random variables to standard normally distributed ones by means of, for example, the Nataf [28] or the Rosenblatt [29] transformation. In the standard normal space, the values of the random variables can be classified into two regions: the safe domain, comprising parameter values, for which a safe operation is possible, and the failure domain, comprising parameter values, for which a prescribed failure criterion is exceeded. The failure criterion can be formulated with respect to the random variables $\boldsymbol{z}$ by means of a performance function $g(\boldsymbol{z})$, where $g(\boldsymbol{z}) < 0$ indicates failure. The most probable point (MPP) is the point with the shortest distance to the origin that lies on the separation curve between the safe and the failure domain. This separation curve $g(\boldsymbol{z}) = 0$ is called limit state function [26]. By means of the MPP, the failure probability P_f for a linear limit state function is given by the first order reliability method (FORM) [26]:

$$P_f = \Phi(-\sqrt{\boldsymbol{z}_{\mathrm{MPP}}^T \boldsymbol{z}_{\mathrm{MPP}}}) = \Phi(-\beta) \tag{1}$$

where Φ is the standard normal distribution function and $\boldsymbol{z}_{\mathrm{MPP}}$ is a vector containing the coordinates of the MPP.

The FORM analysis works well for several (for example, up to 10) random variables and yields correct results if the limit state function behaves nearly linear in a sufficiently large region around the MPP. For more curved limit state functions, the Second Order Reliability Method [30] might be an alternative.

2.3.3. *Numerical methods*

Numerical estimations for the failure probability are based on Monte Carlo simulations (MCSs) [27] or stochastic approaches [24].

A direct MCS generates samples $\boldsymbol{z}_i (i = 1, \ldots, N)$, for the random variables and estimates the probability of failure from several simulation runs. A stochastic approach generates samples of space–time wind distributions according to the turbulence characteristics of the specific site and estimates the probability of failure of the dynamic response of a train crossing the wind field through several simulation runs (overcoming of the overturning threshold [24]). The defined probability of failure can be therefore combined with the probability of occurrence of the wind on the considered site to compute the overturning risk.

However, for small failure probabilities, direct MCS need a prohibitively large amount of simulation runs. An alternative is importance sampling, where the samples are drawn from another probability density function $f(x)$ and weighted by the ratio $p(x)/f(x)$. A good choice for $f(x)$ is to shift the original probability density function to the MPP and eventually to rescale it. Line sampling [31] is another way to obtain estimates for the failure probability with few simulations only. Given a direction vector $\boldsymbol{e}_\alpha$ from the origin to the MPP (for example, from the FORM analysis), every sample is decomposed perpendicular and parallel to $\boldsymbol{e}_\alpha$:

$$\boldsymbol{z}_i = \boldsymbol{z}_i^{\perp} + (\boldsymbol{z}_i^T \boldsymbol{e}_\alpha)\boldsymbol{e}_\alpha. \tag{2}$$

Then, a distance c_i is determined, for which $g(\boldsymbol{z}_i^{\perp} + c_i \boldsymbol{e}_\alpha) = 0$. From this distance, the probability $p_i = \Phi(-c_i)$ is computed, which can be interpreted as the failure probability for the associated one-dimensional problem, i.e. under consideration of direction $\boldsymbol{e}_\alpha$ when the shift $\boldsymbol{z}_i^{\perp}$ is given. The probability of failure is then determined, by taking the average:

$$P_f = \frac{1}{N} \sum_{i=1}^{N} p_i. \tag{3}$$

2.3.4. *Sensitivity methods*

A sensitivity analysis investigates the influence of input parameters on the output of a system. There are local and global methods which differ by accuracy, computational effort and insight into the system. Local methods are computationally less expensive, but give less information about the system. On the other hand, global methods are numerically demanding, but yield averaged values over the whole parameter space.

A semi-analytical, local result can be derived from previous FORM computations. Differentiating β with respect to $\boldsymbol{z}$ at the MPP yields

$$\left.\frac{\mathrm{d}\beta}{\mathrm{d}\boldsymbol{z}}\right|_{\boldsymbol{z}_{\mathrm{MPP}}} = \frac{\boldsymbol{z}_{\mathrm{MPP}}}{\boldsymbol{z}_{\mathrm{MPP}}^T \boldsymbol{z}_{\mathrm{MPP}}}. \tag{4}$$

To investigate the global influence of the excitation and design parameters, the correlation matrix for the performance function $g(\boldsymbol{z})$, with respect to these variables, can be computed

and also a principal component analysis concerning the calculated correlation matrix can be undertaken [32]. A global method, which is less numerically costly than correlation analysis, and which gives also a good insight into nonlinearities of the system, is the Morris method [33]. In the space of all parameters, random walks are performed varying, always, one factor at a time and computing the finite differences:

$$d_i = \frac{g(z_1, \ldots, z_i + \Delta z_i, z_{i+1,\ldots,} z_n) - g(\boldsymbol{z})}{\Delta z_i} \tag{5}$$

with respect to each parameter. The mean values of the norm of these differences show the global influence of the parameters and the standard deviations are measures of the nonlinear effects of these parameters.

3. Experimental techniques

The probability of failure for what concerns the vehicle overturning is usually taken as the probability that the vehicle dynamics overcomes a threshold representing the 90% of wheel unloading (see Section 7.1). In order to determine if the threshold is overcome, the mechanical response of the vehicle under wind loads has to be predicted. For every cross-wind aspect, the definition of the cross-wind loads is necessary and it is usually performed by experimental tests (in wind tunnel or at full scale) or by CFD computations (see Section 4).

3.1. *Wind tunnel tests on trains in cross-winds*

Wind tunnel tests on scaled train models are carried out to measure the aerodynamic forces acting on the leading cars and trailer cars of trains of various sorts. The most common research activities are related to drag reduction, cross-wind, slip stream, internal flows, thermal aspects, aerodynamic noise and other specific topics. In the following, we will discuss wind tunnel testing specifically to assess cross-wind issues.

Unlike the techniques commonly used in the automotive field, where vehicles are tested, in most of the cases, at full scale, with a stationary car on a flat moving ground with boundary layer suction, wind tunnel tests on trains are usually performed on stationary scaled models on different still ground scenarios. Different kinds of wind tunnels can be used: atmospheric [34,35], pressurised [36], closed test section [37], open tests section [37], slotted walls, all aiming at a compromise between the request of large models allowing for a better geometrical detail reconstruction and high Reynolds numbers, and low values of wind tunnel blockage. Train model dimensional scales usually range between 1:100 and 1:7, while the Reynolds numbers of the wind tunnel experiments are between 2×10^5 and 1×10^6.

The simplest ground scenario (perhaps most extensively used in Germany) is the 'flat ground' (FG) since it represents the ground configuration specified in the national standard on cross-wind effects on trains. No aspects of the railway track are modelled. For the sake of reproducibility, a splitter plate or a boundary layer suction facility are used to limit the effect due to the presence of a wind tunnel floor boundary layer whose characteristics depend on the wind tunnel plant. Considering a train moving on an embankment or on a viaduct, the geometry of the scenario becomes significant compared with the train dimension, and the aerodynamic is influenced by the train/ground scenario geometry. Wind tunnel tests on embankment and viaducts have been performed to investigate the differences with the FG configurations. Due to the large differences in the embankment geometry (slope of the side walls and height), adopted in different countries, and in different points of railway lines within the

same country, an attempt to derive empirical formulae, so as to predict the aerodynamic loads on a train vehicle on a generic embankment geometry starting from a reference embankment geometry [34,35] has been made. As a reference embankment geometry, a 6-m embankment is considered whose geometry is given in Figure 3. Other kinds of ground scenarios have been considered by different research groups in different countries, leading to a widespread number of aerodynamic data sets that show similar global aerodynamic behaviours but that are hard to compare due to the differences in the experimental test conditions (see, for example, the double track geometry used in the UK shown in Figure 4).

An attempt to standardise the wind tunnel tests is now ongoing [7,8] and a reference scenario called 'single track ballast and rail' (STBR) has been proposed as the only ground scenario that should be considered. The new reference scenario, whose geometry is shown in Figure 5, has been chosen in order to overcome the over simplification of the FG scenarios in the undercar body region and to overcome the uncertainties of the wind tunnel 6-m embankment results. The geometry of the STBR is aimed at making the wind tunnel results less sensitive to the different flow conditions close to the floor wall that are characteristic of the different wind tunnel test conditions and to give a more realistic reproduction of the flow in the underbody region. Wind loads on vehicles are commonly expressed by means of aerodynamic coefficients as follows:

$$F = \frac{1}{2}\rho A C_{\mathrm{F}} V_{\mathrm{rel}}^2 \tag{6}$$

$$M = \frac{1}{2}\rho A h C_{\mathrm{M}} V_{\mathrm{rel}}^2 \tag{7}$$

where F is a generalised force and$M$ is a generalised moment, ρ is the density of air, A is a reference area and h is a reference height. In Equation (6), V_{rel} is the wind speed relative to the vehicle. In the following, a 'standard normalisation' using the real vehicle dimensions or a 'TSI normalisation' with $A = 10\,\mathrm{m}^2$ and $h = 3\,\mathrm{m}$ is adopted.

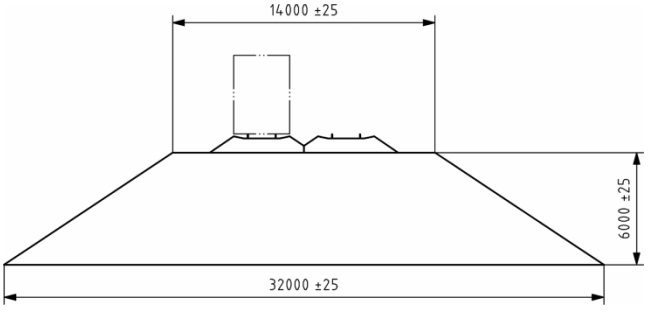

Figure 3. Standard embankment geometry (dimensions [mm]).

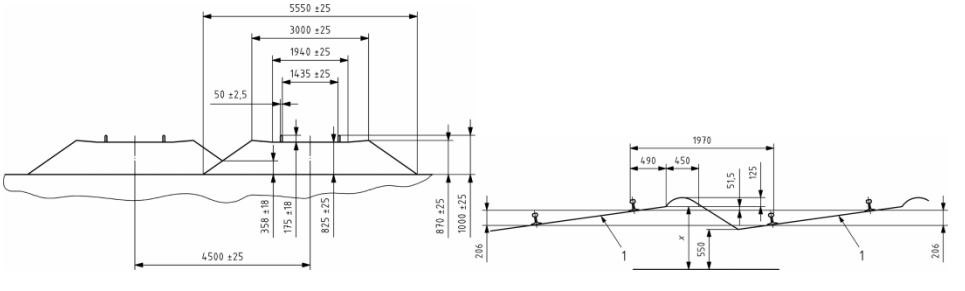

Figure 4. Double track ballast and rails (left), saw tooth canted ballast and rail (right) (dimensions [mm]) [38].

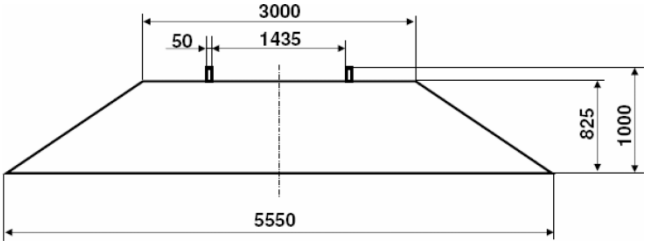

Figure 5. Single track ballast and rail geometry (dimensions [mm]) [7,8].

Tests for measuring aerodynamic coefficients are usually carried out in low turbulence conditions (nominally 'smooth flow'), but the effects of the atmospheric boundary layer and of the wind spectrum frequency content are sometimes required, particularly for slow-moving vehicles, where the effects of vehicle motion are small and the train is subject to large turbulence wind velocity fluctuations. For such tests it is necessary to simulate the atmospheric boundary layer within the wind tunnel [39]. This involves the correct simulation of velocity and turbulence intensity profiles at large scale ($>$1:50) and also the simulation of large turbulence length scales. A typical test configuration in the Politecnico di Milano (PoliMi) boundary layer wind tunnel is shown in Figure 6 and a simulated wind spectrum is shown in Figure 7 [39].

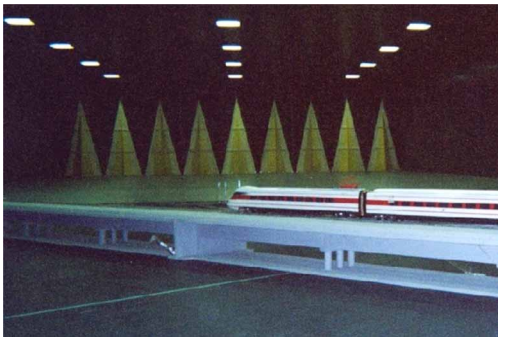

Figure 6. Turbulence-producing spires placed before the test section.

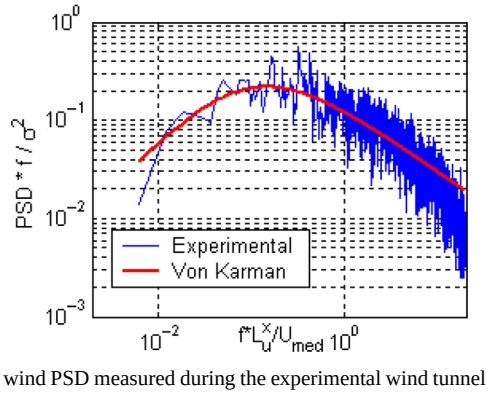

Figure 7. Non-dimensional wind PSD measured during the experimental wind tunnel tests compared with those of the Von Karman.

Stationary wind tunnel tests do not correctly model the relative motion between the train and the ground, and a number of experiments have been carried out to investigate the effects of moving models on aerodynamic forces and moments. The earliest of these is described in [40], where 1:50 scale models of the UK Advanced Passenger Train were catapulted across a wind tunnel in which an atmospheric boundary layer had been simulated. Perhaps the most important point to emerge from these tests was the realisation that to obtain stable mean values of the measured forces and moments, the average results from a large number of identical tests were required. More recently, moving scaled model of the ETR480 train was used at the wind tunnel at PoliMi instrumented with an internal balance to measure the forces acting on the train model while it crosses the wind tunnel flow [39]. A picture of the experimental rig is shown in Figure 8. The train model is released from the top of a ramp and runs on a track accelerating, due to gravity, in the initial part where the track is inclined. It passes through a tunnel and it reaches the horizontal part of the track, where the measurement is made in order to simulate the sudden variation of the wind action at tunnel exit [39].

3.2. *Wind tunnel tests on road vehicles*

Wind tunnel tests on heavy vehicles are in many ways similar to those already presented for trains but little work in this field has been reported in the literature. Wind tunnel tests have been carried out on 1:10 scale models of different heavy vehicles (truck, lorry with trailer and tanker) considering three infrastructure scenarios (FG, viaduct and embankment) at the Politecnico di Milano wind tunnel, both with and without boundary layer simulation. Pictures of the models are shown in Figure 9. Further tests have been carried out recently as part of the EU sponsored WEATHER project [41], and these results have been compared with the results of full scale testing and CFD calculations (see Sections 5 and 6).

3.3. *Full-scale experiments*

Full-scale experiments are, by their nature, complex to carry out, requiring both sensitive yet robust instrumentation, and also relying on the vagaries of the natural wind. It is also found that there is, very often, a large spread of data, due to the uncontrolled nature of the wind conditions, that require very careful handling to produce meaningful results. Nonetheless, a number of full

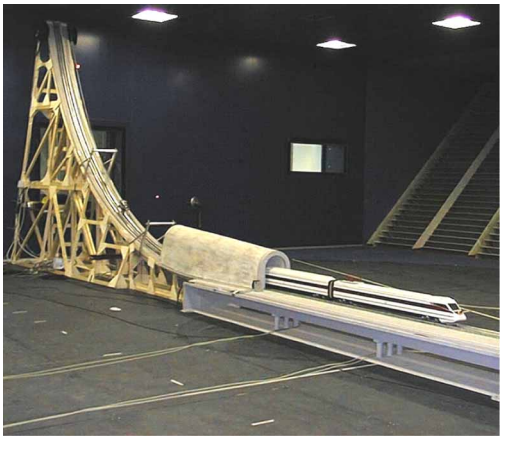

Figure 8. Moving model tests in the PoliMi wind tunnel.

Figure 9. Scale vehicle models: van (left); tanker (centre); truck (right).

scale experiments have been attempted in the past – the full scale measurements in Germany on a moving Inter-Regio train as part of the TRANSAERO project [42], stationary full scale tests in the UK on the Class 390 Pendolino [43], tests in Japan on a train type JR103 [44] and the recent EU-funded WEATHER project that measured wind forces on a stationary and a moving high-sided vehicle [41].

4. Computational techniques

Nowadays CFD is well established in the design process of road and railway vehicles. CFD is used, for example, to calculate and optimise aerodynamic drag, head pressure pulse, and the aerodynamic forces and moments under cross-wind conditions.

The homologations of trains related to cross-wind stability currently rely on static tests from wind tunnels, described in [7]. Thus, most of the related numerical work is focused on reproducing a configuration found in static wind tunnel tests. Numerous investigations were made in particular in the DEUFRAKO Cross Winds project, dealing with high-speed trains that serve as reference for the European homologation process. A good correspondence is often found for small yaw angles (relative wind angles). Only recently there are attempts to capture more realistic configurations including gust models with CFD [45,46].

The simulation of road vehicles encountering cross-wind is also common in the automotive sector. The focus, here, is to mimic as much as possible realistic conditions, which is the motivation to include gusts in the determination of the aerodynamic coefficients [47]. The motivation to take into account gusts for road vehicles stems from the vital interest to determine not only the risk of overturning but also the risk of side-slip and related counter steering, which is a function of the time-dependent forces and moments acting on the vehicle.

The choice of the CFD method should depend on the configuration, the geometry of the vehicle, the boundary conditions chosen and the goal of the investigation. The popularity of RANS methods, within the engineering community, can be attributed to the fact that they deliver directly time averaged results which are sufficient for most engineering applications. Today, the homologation of trains requires only mean aerodynamic coefficients in contrast to the automotive sector, where realistic driving conditions and therefore time-dependent turbulent effects are getting more and more attention. For cross-wind stability investigations, RANS methods are usually sufficient for flow topologies where the turbulent scales are, at least, one order of magnitude smaller than the characteristic length of the flow problem. This is typically found at streamlined vehicles subjected to small yaw angles. Non-streamlined vehicles typically produce detached vortices, which in turn counteract on the mean flow (back scatter). Therefore, the predictive accuracy of RANS methods drops significantly for high yaw angles, especially in combination with vehicles exhibiting protruding objects at the roof which, in turn, provoke detached vortices. For this type of flow it is advisable to revert to inherently transient methods as large eddy simulation (LES), detached eddy simulations (DES) or simulations

based on the Lattice–Boltzmann formulation. Those methods are principally superior compared with RANS methods as they require less empirical input and deliver information about large-scale turbulent spectra. Time-dependent methods are also required if time-dependent boundary conditions, like gusts, cause significant hysteresis effects due to turbulence restructuring and if the dynamic response of large scale structures on the aerodynamic coefficients is required as input for vehicle dynamics. Some authors also use unsteady RANS (URANS) methods with the drawback of usually low diffusivity and resulting artificially high coherence of the vortices due to non-resolved fine-scale turbulence. Theoretically, the easiest way to simulate a cross-wind would be to use a direct numerical simulation, which means to resolve simply the Navier–Stokes equation without the need for turbulence modelling and near-wall treatment (see Figure 10). However, such a computation would be not feasible on today's computers due to the extremely high number of grid points required ($\sim \mathrm{Re}^{9/4}$) in order to resolve all turbulent scales. The Reynolds number is around 1 million in most of the wind tunnel experiments and 10 million in reality, based on the width of the train.

4.1. *Potential theory*

Potential theory solver can be used for flow types where non-viscous and non-rotational flow regions dominate the problem. An example for a suitable type of problem is the head pressure pulse for streamlined vehicles which has been presented by Mackrodt and Pfizenmaier [48]. However, a vehicle running under cross-wind conditions exhibits extended regions of separated flow and the position of the separation line is usually dependent on the boundary layer development. The fact that those phenomena cannot be modelled with a solver based on potential theory usually prevents engineers to use this model for cross-wind stability. However, Chiu [49] used such a method for cross-wind simulation but restricted his investigation to extremely high yaw angles ($<60°$), where three-dimensional separation plays a subordinate role.

4.2. *Reynolds-Averaged Navier–Stokes*

Flow solvers based on the Reynolds-Averaged Navier–Stokes (RANS) equations are the most commonly used technique in industry for the prediction of the aerodynamic coefficients of vehicles under cross-wind effects. The basic idea behind this technique is to split the flow field variables u into a mean part $\langle u \rangle$ and a fluctuating turbulent part u' : $u = \langle u \rangle + u'$. The resulting time-averaged Navier–Stokes equations lead to new terms called Reynolds stresses, which are then usually modelled with linear or non-linear eddy viscosity models. The k-ε model was introduced by Pantakar and Spalding [50] and applied to vehicle aerodynamics by Markatos [51]. Another wide-spread two-equation model is the k-θ model, which is believed to behave better in the near-wall region compared with the k-ε model, which is usually better

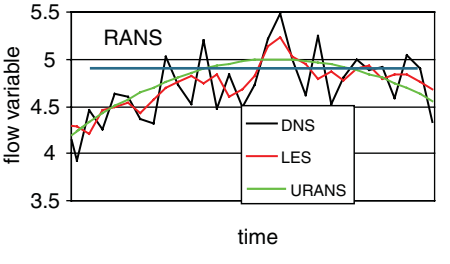

Figure 10. Comparison between different CFD approaches.

suited for free stream flow. This motivated Menter [52] to introduce the so-called SST model, which combines both approaches with a set of empirical blending functions. More sophisticated Reynolds Stress models [53] require the transport and solution of the turbulent stresses. This enables an improved formulation of the turbulent production terms, and in contrast to eddy-viscosity models, they could principally reproduce the anisotropy of the turbulent stress which should be particularly important for an improved turbulence modelling of the longitudinal vortices produced at the lee-ward side of vehicles running under cross-wind conditions. One of the advantages of RANS methods is the vast experience gained in the last decades with a quite big number of investigations and validation against experimental data. Examples of recent studies of cross-wind stability of railway vehicles using RANS are found in TRANSAERO project [54–57]. RANS methods are also widely used in the automotive sector. Guilmineau and Chometon [47], Ryan and Dominy [58] and Juhlin and Eriksson [59] represent studies using generic car configurations to investigate cross-wind effects.

4.3. *Large eddy simulation*

LES methods solve the spatially-averaged Navier–Stokes equations. The flow variables are split into a term $\langle u \rangle$ (representing the part of the flow that can be discretised within the given computational mesh) and a term u' (which represents the fluctuations that are not captured by the grid due to their small size). The non-resolved part of the flow is thus modelled through a so-called subgrid scale model, which determines the so-called turbulent viscosity. Thus, the resulting viscosity is the sum of the turbulent viscosity and the molecular viscosity of the flow. Most of the turbulence models used in vehicle aerodynamics applications are based on a formulation with the so-called Smagorinsky constant C_s, which is dependent on the type of flow and has been determined to be $C_s = 0.23$ for homogenous turbulence by Lilly [60]. A useful extension of this model has been introduced by Germano [61]. This extended model is called dynamic model, as it determines the Smagorinsky constant out of the actual flow situation. The advantage of the dynamic model approach is that no a priori assumption is needed for the determination of the Smagorinsky constant. LES models are principally suitable for the simulation of vehicles subjected to cross-wind also for high yaw angles exhibiting transient flow with detached eddies. The disadvantage of LES is the rather big number of grid points necessary to resolve the boundary layer. This might be the reason why only a small number of publications promoting this method are found in the literature.

4.4. *DES*

DES models are using a RANS formulation for the boundary layer region and an LES formulation for the rest of the flow field. This hybrid scheme allows combining the advantage of both methods and is becoming quite popular also in the industrial context [55,62].

4.5. *Lattice–Boltzmann*

The Lattice–Boltzmann method [63] is a powerful technique for the computational modelling of a wide variety of complex fluid flow problems including single and multiphase flow in complex geometries. It is a discrete computational method based upon the Boltzmann equation. It considers a typical volume element of fluid to be composed of a collection of particles that are represented by a particle velocity distribution function for each fluid component at each grid point. The time is counted in discrete time steps and the fluid particles can collide with each other as they move, possibly under applied forces. The rules governing the collisions are

designed such that the time-average motion of the particles is consistent with the Navier–Stokes equation [64].

5. The pressure distribution and flow field around rail and road vehicles

5.1. *High-speed trains*

5.1.1. *Flow field around vehicles*

In the last few decades, a number of wind tunnel tests and computational simulations have elucidated the flow structure around high-speed trains in cross-winds. The wind tunnel work of [49,65–67] in the 1970s and 1980s used an idealised train model, and it was found that the dominant flow pattern was a series of inclined wake vortices such as might be found around a missile at high angles of attack (Figure 11a). At higher yaw angles, a more conventional vortex shedding pattern was observed, with some switching of the flow at intermediate angles. Recent computations, using both RANS and LES techniques, on various ICE configurations [50,55,64] have also shown similar patterns (Figure 11b and d). There is broad agreement both qualitatively and quantitatively between the wind tunnel tests and the CFD

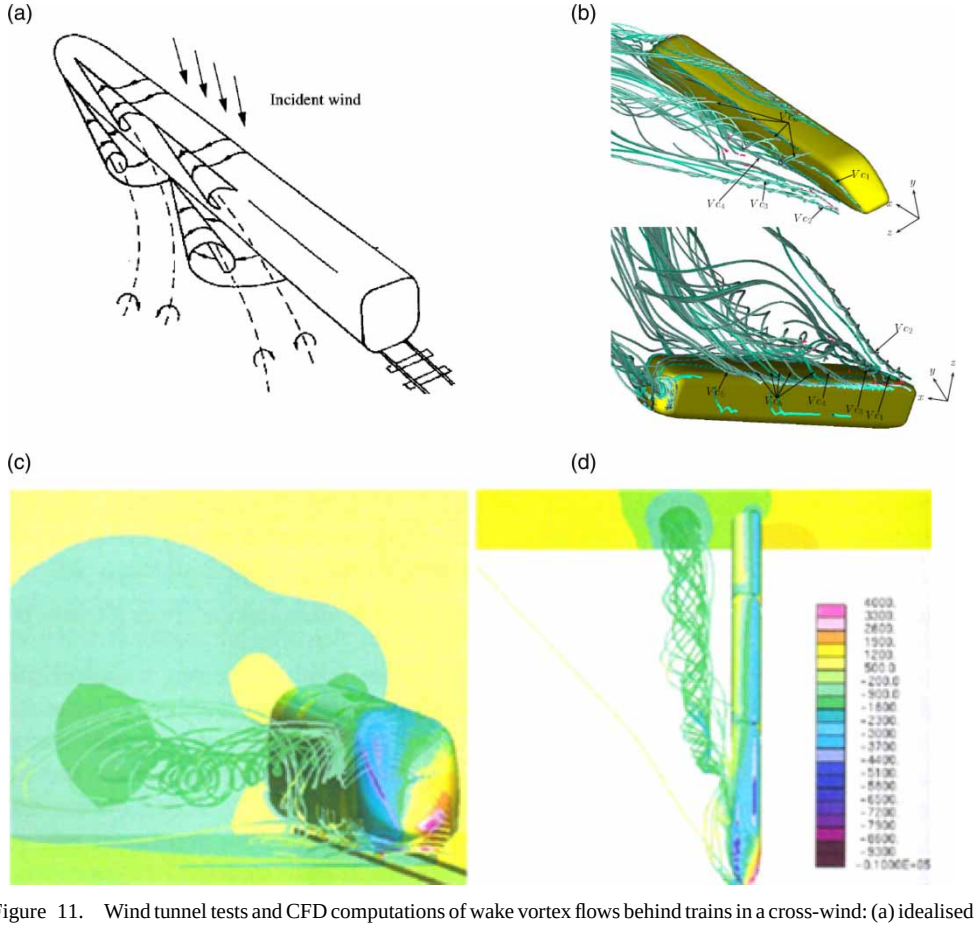

Figure 11. Wind tunnel tests and CFD computations of wake vortex flows behind trains in a cross-wind: (a) idealised train [68]; (b) car ICE [56]; (c, d) ICE [57].

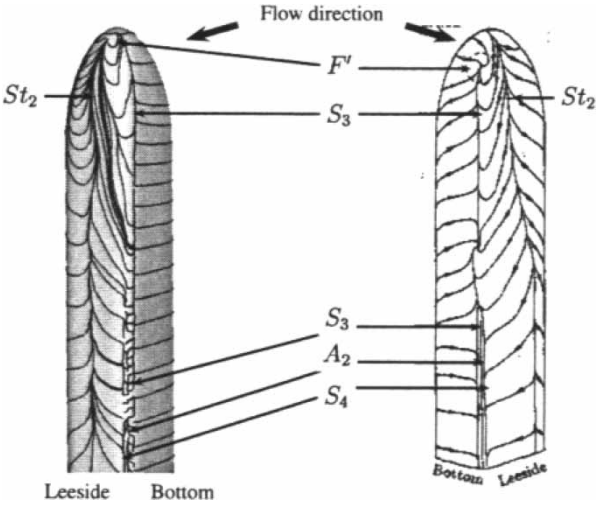

Figure 12. Computed and measured surface streamline patterns [49,56].

results (see the surface streamline patterns in Figure 12). There is some evidence, particularly from the LES results of wake unsteadiness [64], that indicates two modes of wake unsteadiness – a horizontal wake oscillation with a Strouhal number of 0.1, and a weak vortex shedding motion with a Strouhal number of 0.15–0.2. It has to be said, however, that these frequencies are not always well defined in the LES simulations, and do tend to vary somewhat with the type of calculation used.

Measurements of a different kind are reported in [15], which presents data from moving model experiments on a four car ICE train, with rather a crude cross-wind generator placed normal to the moving model track. The x axis unit is time-normalised by train velocity and carriage length – with 0 being the point at which the train nose passes the measurement point, and 4 being the point at which the train tail passes that point. The y axis is the slipstream velocity normalised by the train velocity. The slipstream velocities were measured in the wake of the vehicle. These results are shown in Figure 13 in two formats – one for the velocities themselves (Figure 13a) and one for the velocities minus the velocities measured with no cross-wind (Figure 13b). In the first of these, the cross-wind magnitude maximum can be seen before the train nose has passed, and the inviscid nose peak is clearly visible. This is followed by a dip in the velocities, due to the sheltering effect of the train. A maximum in the velocity can then be seen before a gradual decay. In the wake, the cross-wind velocities are again seen. In the alternative method of presentation, any value of the relative velocity that exceeds the upstream wind speed indicates an enhancement of that wind speed by the train wake. This can be seen to occur at a position that corresponds to the passing of the second car of a four cartrain, with lower values elsewhere. Baker *et al*. [15] argues that this is consistent with the presence of inclined vortices in the wake of the four car train. Finally Figure 14, again from [15], shows the maximum wake velocities (one second averages) that were measured for a wide variety of high-speed trains in full scale test in the UK, normalised by the train speed. There is, inevitably, a great deal of scatter, but it can be seen that there is a general increase in the maximum normalised velocities as the cross-wind speed increases.

5.1.2. *Pressure distributions*

The idealised train low turbulence wind tunnel measurements of Chiu [49], Mair and Stewart [65] and Copley [66], made extensive measurements of the pressure distributions

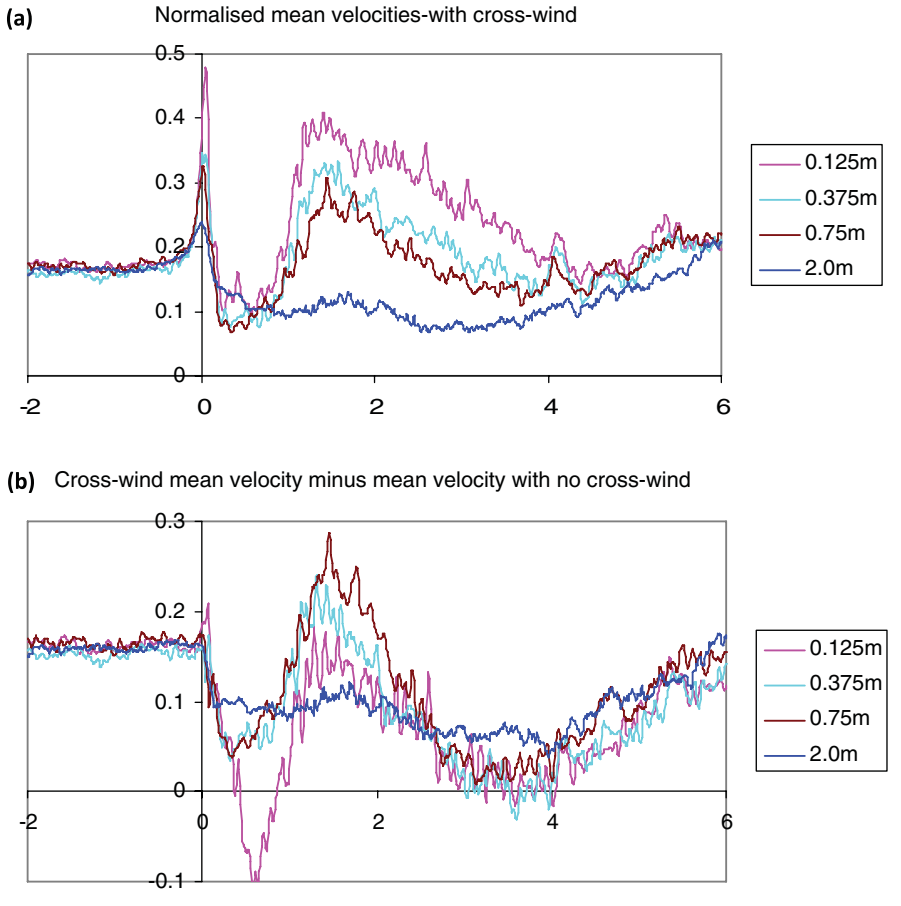

Figure 13. Wake velocity measurements from moving model experiments for ICE model [17].

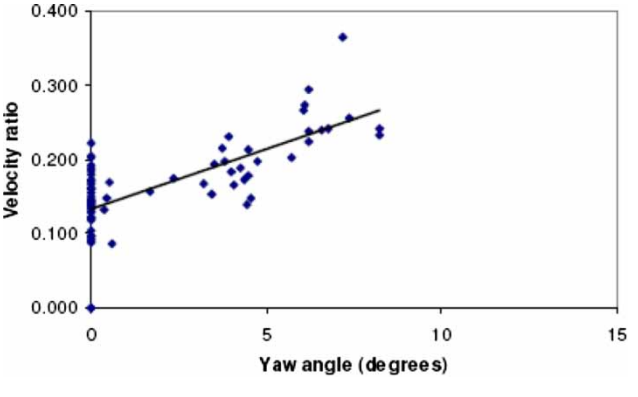

Figure 14. Maximum slipstream velocities for high-speed passenger trains [17].

around the model, and sample results are shown in Figure 15a [49] together with the results of simple panel method calculations. Figure 15b shows equivalent measurements for a two car ICE 2 model [69], which also shows the LES calculations of [55]. Pressure coefficients are shown on loops around the vehicle, for a variety of different distance (x) from the train

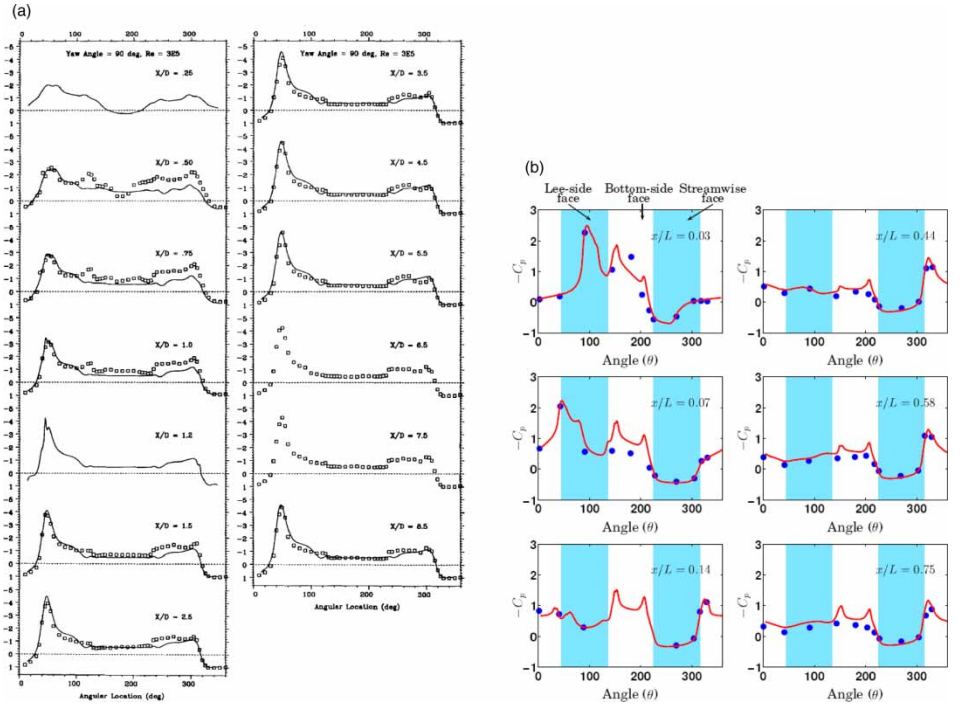

Figure 15. Pressure distributions around trains: (a) idealised train – lines represent panel method results and points depict experimental results [49], front of windward face is at 0°; (b) car ICE – lines indicate LES results of [69] and points show the experimental results of Wu [55], front of windward face is at 270°.

nose, normalised with the model diameter D or length L. The results are plotted with a negative pressure coefficient in the positive direction. For all values of x that are not near the nose, it can be seen there is a suction peak on the windward roof corner (45° in Figure 15a; 315° in Figure 15b), small suctions over the rest of the roof, leeside and underside, and a positive pressure coefficient on the windward wall. Near the nose however, for small values of x there is a suction peak on the leeward side, that can be expected to give a major contribution to the overall side force. In general, the numerical solutions show a good level of agreement with the experiments.

5.2. *Road vehicles*

5.2.1. *Flow field*

The flow field around road vehicles in cross-winds has been much less extensively studied than the flow field for trains. For those vehicles, where cross-wind effects are most significant (high-sided vans and lorries), it can be expected that the wake flow around such vehicles in a cross-wind will be very disorganised, as the vehicles are in, aerodynamic terms, three-dimensional bluff bodies with large scale wake separation. For such bodies, there are unlikely to be coherent wake flow structures as around trains, and thus there are unlikely to be any regular wake oscillations. On the roof of the vehicle, some investigations have inferred, through surface flow visualisation, the presence of ‘delta wing’ conical vortices in the vicinity of the windward corner of the vehicle ([70], see Figure 16). Such vortices produce high suctions on the surface beneath them and can lead to high lift.

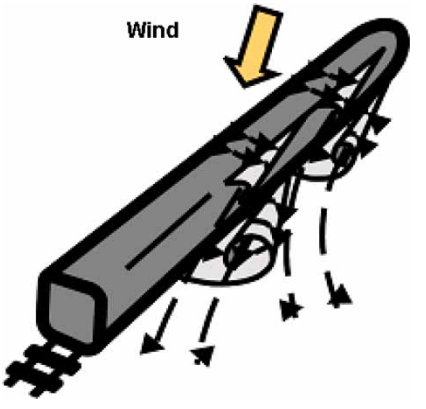

Figure 16. 'Delta wing' conical vortices in the vicinity of the windward corner of the vehicle.

5.2.2. *Pressure distributions*

Sterling *et al.* [41] reports surface pressure measurements on a large box van from full-scale experiments, atmospheric boundary layer wind tunnel experiments and RANS CFD calculations, and some of the results are shown in Figure 17 for a yaw angle close to 90°. It can be seen from the full-scale results how the pressure distribution is similar to that on a full-scale building, with a positive pressure on the front face, a high suction near the windward roof corner, and low suctions over the rest of the roof, the leeward side and the underbody. The same authors show that the wind tunnel tests produce these trends quite well [41], although the magnitudes of the pressures are not always close. The CFD results however fail to fully predict the large suction peak on the roof of the vehicle, although the windward and leeward face pressures are well predicted.

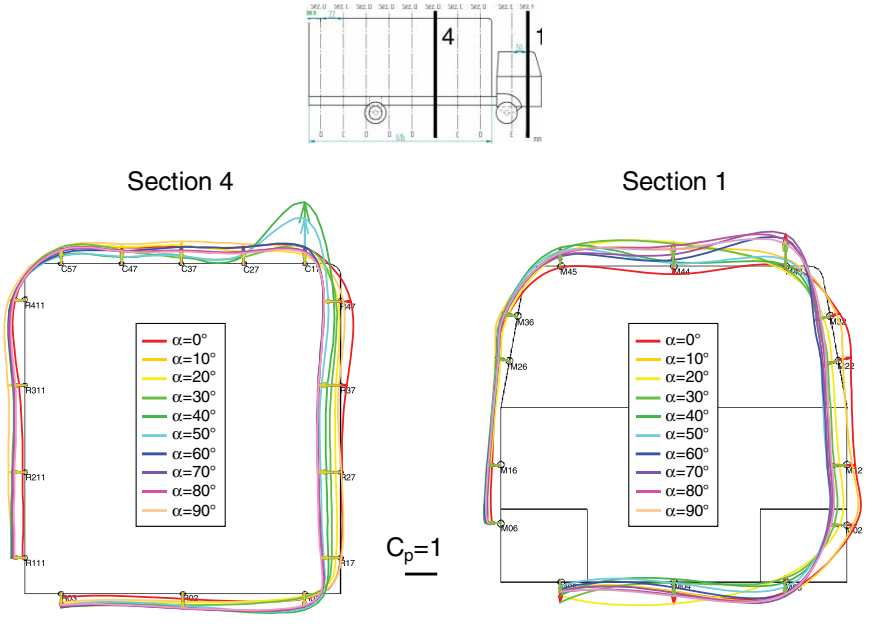

Figure 17. Surface pressure measurements on a large box van from full-scale measurements.

6. Steady and unsteady aerodynamic force and moment parameters

6.1. *Force and moment requirements for risk calculations*

It will be seen in Section 7 that the aerodynamic forces and moments required for risk calculations are rather different for rail and road vehicles. For rail vehicles, generally, only the rolling moment about the leeward rail is required for overturning risk calculations, in the more simplified approaches, although if the behaviour of the vehicle dynamic system is being investigated, the side and lift forces will also be required. It is worth noting, however, that the lee rail rolling moment is, basically, the sum of the moments about the lee rail of the side and lift forces. For road vehicle calculations then all six aerodynamic force and moment coefficients are required. For simplicity, in this section we will present various compilations of data for side and lift forces on both road and rail vehicles (expressed in suitable dimensionless forms according to Equations (6) and (7)) and refer the reader to other sources for more detailed data.

Aerodynamic forces and moments can be used in different ways: in the amplitude, frequency or time domain. Amplitude domain calculations usually require the maximum values of the forces and moments. These are usually obtained from force and moment coefficients formed with the mean values of force measured in the wind tunnel and the mean values of wind speed, and from extreme gust values of the wind velocity. This is particularly appropriate for very high-speed vehicles when the vehicle velocity is the major component of the velocity relative to the vehicle and thus the effect of wind velocity fluctuations can be expected to be small. However in some instances, especially when vehicle speeds are low, it is more appropriate to define the coefficients with extreme values of force and extreme values of wind tunnel velocity obtained from an extreme value analysis. This will be discussed further in Section 7.

If calculations are carried out in the frequency domain, the important parameters are the force and moment spectra. A convenient way to specify these parameters is through the parameter known as the 'aerodynamic admittance' X, defined as the ratio between the force spectrum S_F and the upstream wind spectrum S_U:

$$X^2 = \frac{1}{(\rho A V_{rel} C_F)^2} \frac{S_F}{S_U}. \tag{8}$$

Finally, if the force and moment data are used in time domain calculations, the required parameters are usually the coefficients defined with the mean force and the velocity values, and the parameter (known as the 'weighting function'), which relates the wind speed fluctuations to the aerodynamic force fluctuations. This parameter can be shown to be the Fourier Transform of the aerodynamic admittance.

In the following sections, we will present data for the mean force coefficients (Section 6.2), the extreme force coefficients (Section 6.3), the aerodynamic admittances (Section 6.4) and the weighting functions (Section 6.5).

6.2. *Mean force coefficients*

In this Section we will consider the side and lift force coefficients defined with the measured mean values of force and wind speeds for three cases

- high-speed (300 km/h) trains (the DB, ICE and the Italian ETR);
- a conventional (200 km/h) train (the UK Class 390 Pendolino);
- a high-sided van.

Further details of force coefficients for other types of road vehicle are given in [59,71,72] for buses and [68,73,74] for cars. These will not however be considered further here.

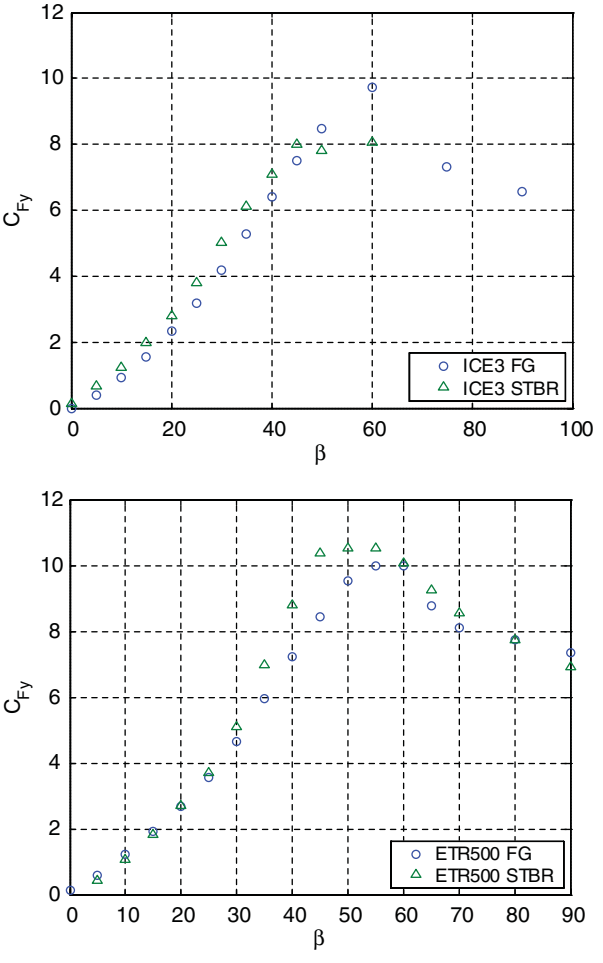

Figure 18. ICE3 and ETR500 Side force coefficients on FG and STBR (TSI normalisation) (β is the yaw angle).

Figures 18 and 19 present a comparison between the side force coefficient measured on the ETR500 and the ICE3 models measured in wind tunnel for different ground scenarios: (FG, single track ballasted rail and 6-m embankment with train model positioned on the windward track or on the leeward track).

Figure 20 presents a comparison of the side force coefficient measured on a stationary and moving ETR480 model [39].

The differences between the FG and STBR case and the moving and static results are small, but the effect of embankment simulation can be seen to be significant and quite variable across the yaw angle range. It will be seen that this effect is one of the major uncertainties in specifying the cross-wind aerodynamic forces and moments on trains.

Figure 21 shows the comparison of different wind tunnel measurements performed on a ICE2 train model at different wind velocity in terms of side force coefficient and lift force coefficient. Reynolds number effects are negligible on the lateral force coefficients while they seem to be more effective on the vertical force coefficient at large yaw angles.

Figure 22 shows a comparison for a variety of different types of CFD simulations and wind tunnel tests on an ICE2 model [37,75].

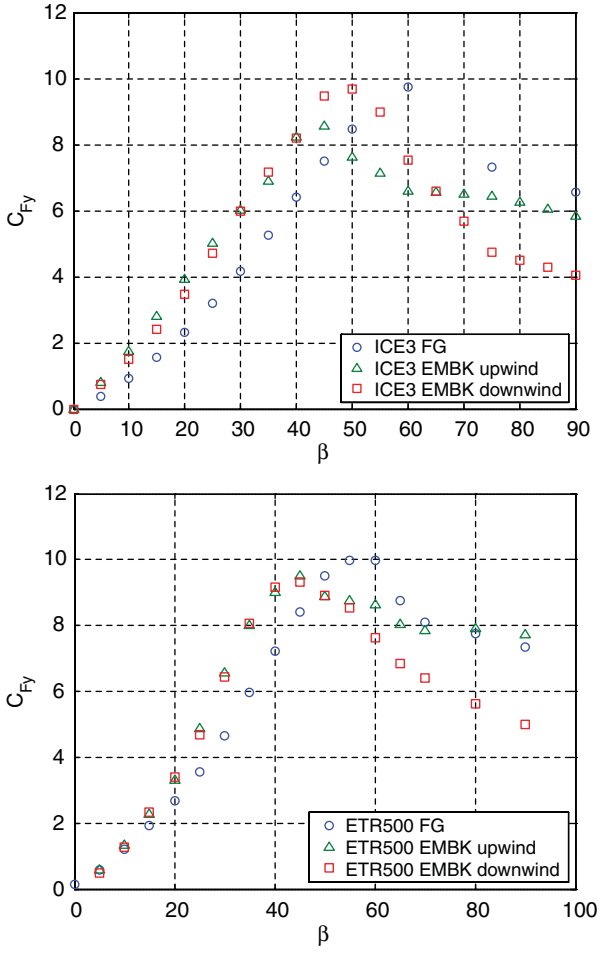

Figure 19. ICE3 and ETR500 Side force coefficients on FG and embankment (TSI normalisation).

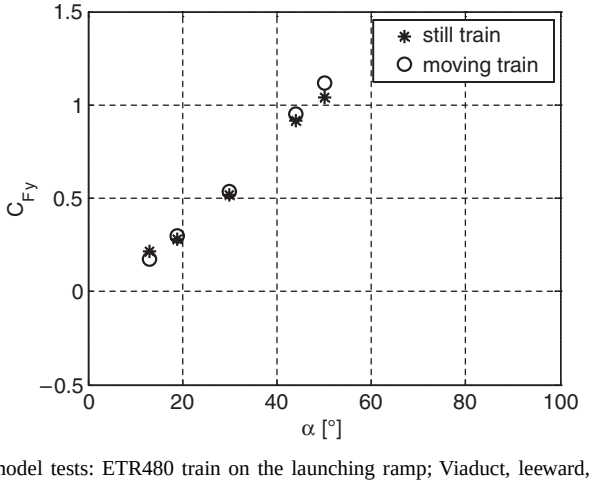

Figure 20. Moving model tests: ETR480 train on the launching ramp; Viaduct, leeward, low turbulence: comparison between side force coefficients measured in still and moving model tests on the leading vehicle (standard normalisation) (α is the yaw angle).

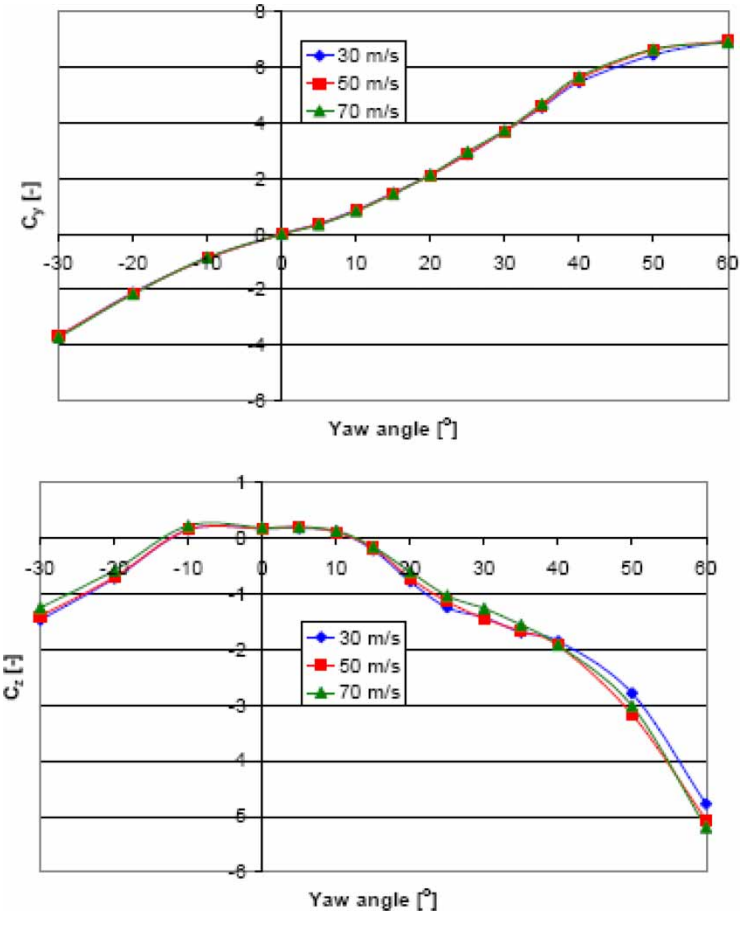

Figure 21. CFD values of side force and lift force coefficients for simplified ICE-2 train at various train speeds (TSI normalisation).

Figure 23 shows a compilation of data for the UK Class 390 Pendolino. This comes from a variety of sources – stationary full scale experiments in natural wind conditions [43]; and stationary wind tunnel experiments with a simulated atmospheric boundary layer [43]. In all cases a FG simulation was used, but with some simulation of the ballast and rail. It can be seen that for the side force coefficient the full scale and the boundary layer wind tunnel results are remarkably consistent with each other, whereas the low turbulence wind tunnel coefficient values are somewhat higher. The lift force coefficient values show considerably more scatter, thus again indicating the sensitivity of this parameter to the precise type of wind tunnel test carried out.

Figure 24 shows a data compilation of the side and lift force coefficients for a large van, which were obtained as part of the WEATHER project [41]. Results are shown from full-scale experiments and wind tunnel tests, both with a simulated atmospheric boundary layer and for CFD RANS computations. Again good agreement can be seen for the side force values, with the lift force values again being more variable.

6.3. *Extreme force coefficients*

In this Section, we consider just one data set (the Class 390 Pendolino) and present the ratio of the side and lift force coefficients formed with extreme (3 s) forces and velocities to those

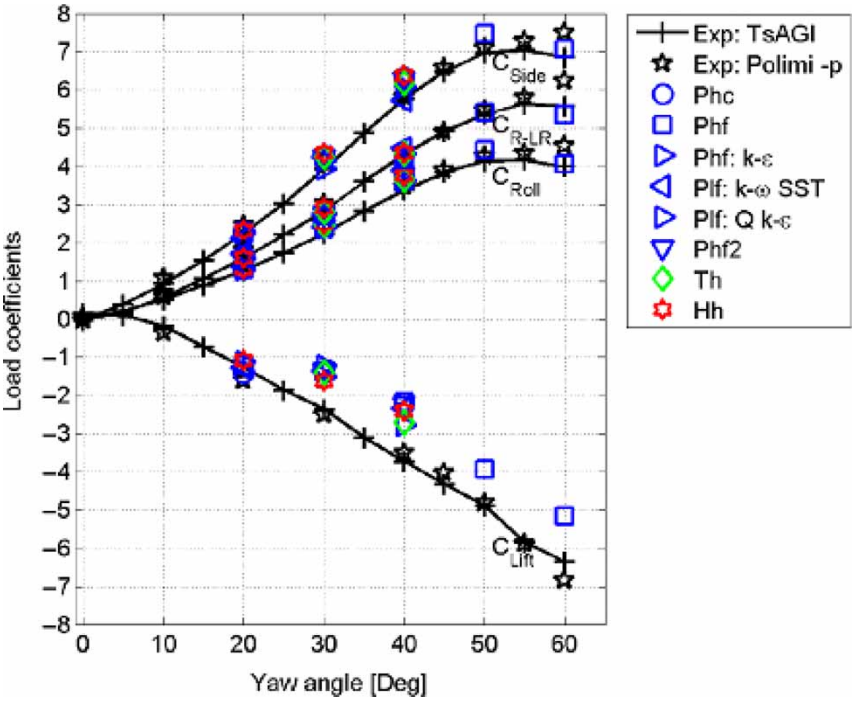

Figure 22. Comparison of wind tunnel experiments and CFD tests for ICE (TSI normalisation).

formed with mean forces and velocities [42]. Results are shown in Figure 25 for full-scale and wind-tunnel tests carried out in atmospheric boundary layer conditions. It can be seen that the values of this ratio are somewhat scattered, but show values of somewhat less than unity at high yaw angles and values of above unity at lower yaw angles.

6.4. *Aerodynamic admittances*

Figure 26 shows a compilation of aerodynamic admittance data from [76] for a variety of different types of vehicle. In general, these curves take on one of two forms: a constant value at low frequency and a gradual fall off at high frequency (indicating the lack of correlation of turbulent fluctuations over the side of the vehicle), and a similar curve, but with a peak in the mid frequency range. The latter type only seems to occur for lift force admittances. The authors suggest that this peak may be either caused by vortex shedding from the vehicle wake, or by force fluctuations attributed to vertical velocity fluctuations. Note that, in principle, the values of the admittance at low frequencies should be unity, which is clearly not the case for all the data shown in Figure 26. This is due to the reference velocity being measured on a streamline that does not impinge directly on the vehicle itself, and thus not fully representing the correct turbulence conditions. In discussing, these authors arrived at the concept of the 'significant streamline': a nominal streamline with turbulence characteristics that are most representative to those around the vehicle.

6.5. *Weighting functions*

As noted above, the weighting function is the Fourier transform of the aerodynamic admittance and can thus be calculated from curves such as those shown in Figure 27 reported for the side

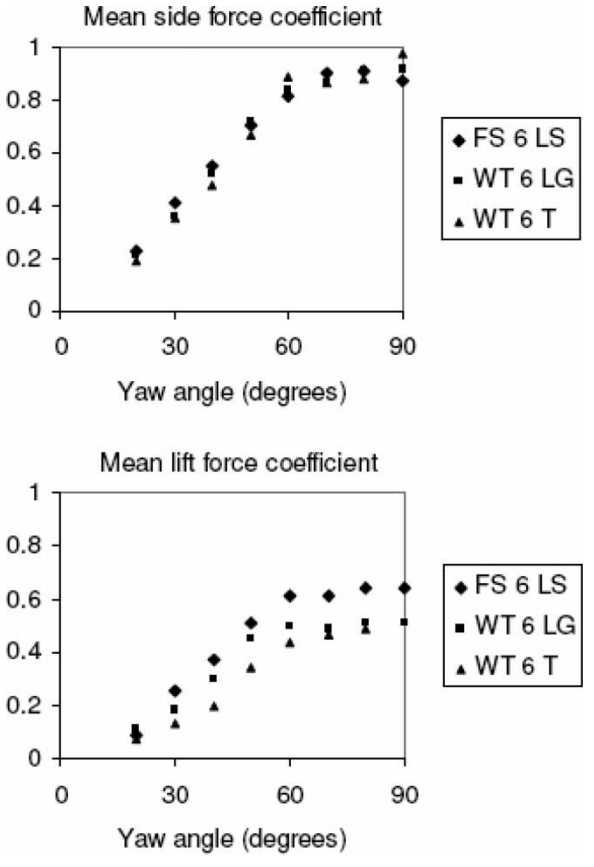

Figure 23. Pendolino data (standard normalisation): FS 6 LS – full scale data at 6° cant; WT 6 LG – wind tunnel data, level ground simulation, 6° cant; WT 6 T – wind tunnel data, full scale topography simulation, 6° cant).

force and lift force. The approach taken by [77] to achieve this has been to fit an analytical curve to the admittance functions (having the form of a two degree of freedom harmonic oscillator characteristic), which has a Fourier transform that can then be found analytically. Following this approach, the two types of admittance function noted above can be shown to have weighting functions of the type shown in Figure 27. It can be seen that for both types, the weighting function decays to zero after a normalised time of 0.6–0.8, corresponding to a real time of around 1 s indicating that the aerodynamic forces react to turbulence velocity fluctuations over the preceding second and not for any greater period. The oscillations in the second type of admittance function also indicate a more coherent periodicity in the forces.

7. Interaction between aerodynamic forces and the vehicle dynamic system

In this Section the interaction of the aerodynamic forces with the vehicle dynamic system will be discussed. From a theoretical point of view, the evaluation of the wind induced effects on the vehicles can be carried out, according to the type of problem (vehicle overturning, comfort, course deviations, and so on), in the frequency domain, in the amplitude domain or in the time domain [78–80]. Both in railway and in road field, during recent years, the main interest has

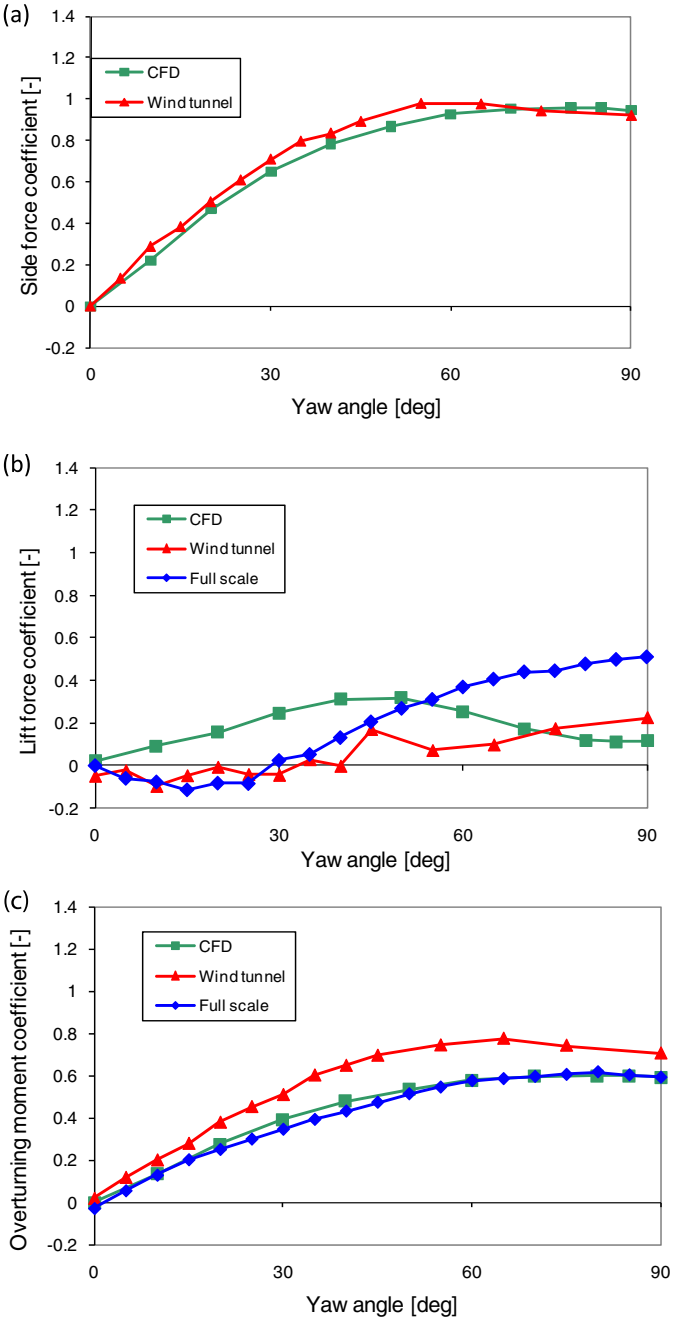

Figure 24. Data from WEATHER project for a large van (standard normalisation): (a) side force coefficient; (b) lift force coefficient; (c) rolling moment coefficient.

been focused on the definition of the limit wind speed that leads to the vehicle overturning. This analysis can be carried out through both a quasi-static approach (amplitude domain) or through a dynamic approach (time domain). Simulation in the time domain is the only one able to account for the effects of both non-linear elements (bumpstops, damping, stiffness) of the vehicle and the contact phenomena between rail and wheel or tyre and road in the vehicle's

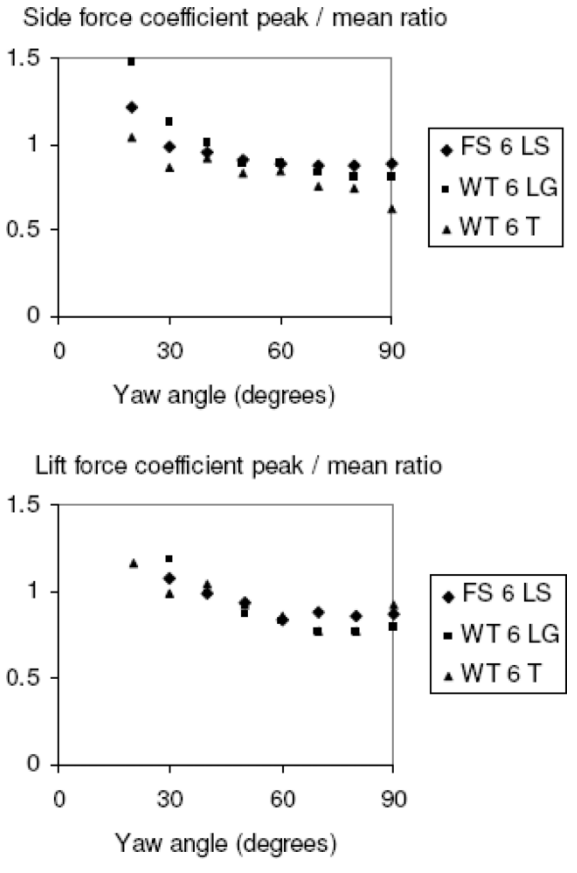

Figure 25. Extreme force coefficients for Class 390 Pendolino.

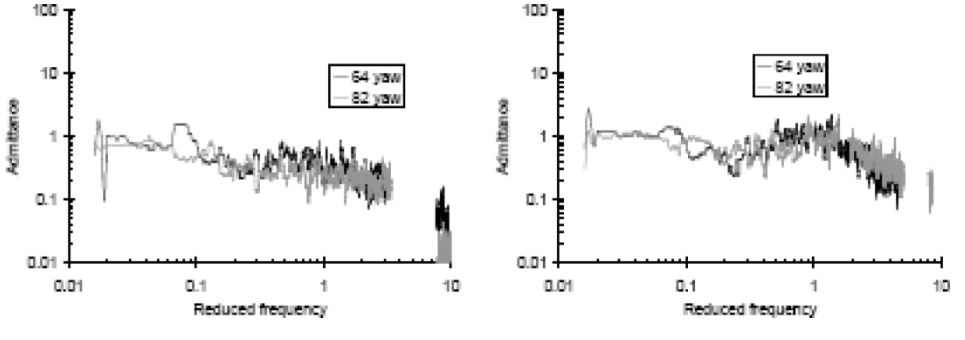

Figure 26. Admittances for Class 390 Pendolino.

dynamic response. Moreover, only through an integration in the time domain of the motion equations of a vehicle subjected to the unsteady aerodynamic forces and moments caused by unsteady cross-winds, it is possible to make an evaluation of a number of effects associated to the cross-wind and not only of the vehicle roll over. In fact, turbulent cross-winds can, in principle, result in a loss in ride quality if specific vibration modes are excited; the lateral

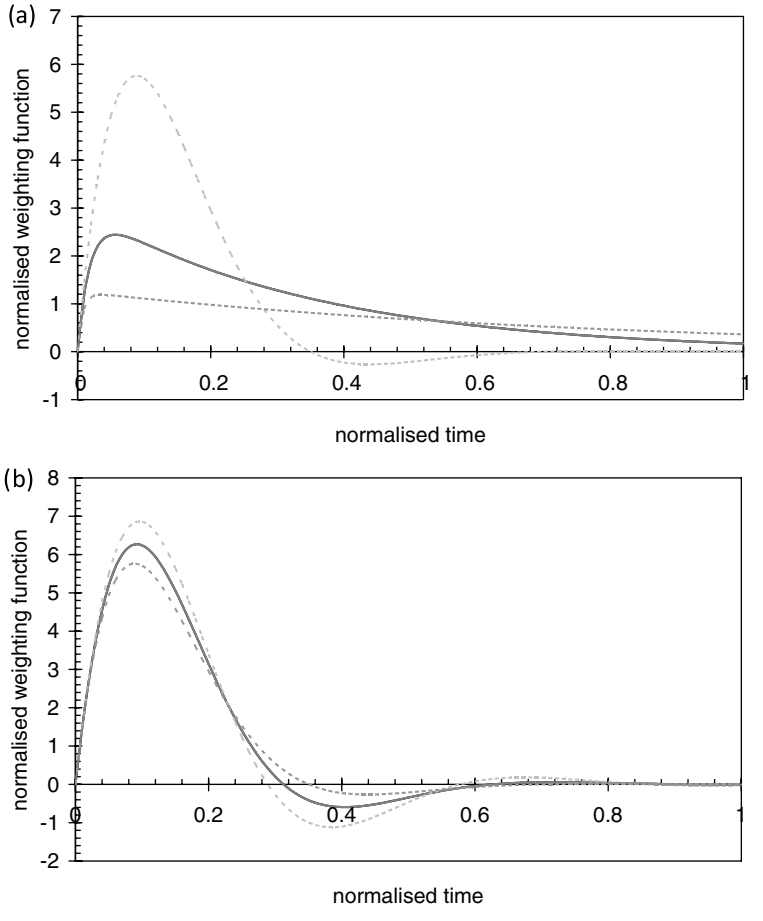

Figure 27. Weighting functions (solid line shows mean value; dotted lines show values from the envelope of aerodynamic admittances): (a) for side force coefficient data; (b) for lift force coefficient data.

displacement of trains in cross-winds can cause the kinematic envelope to be infringed, and can also cause potential dewirement problems with large scale pantograph displacements [13]. However, the time-domain approaches are more expensive and, in some cases, more complex than quasi-static approaches.

7.1. *Quasi-steady methods*

The stationary aerodynamic roll moment about the leeward rail is defined as

$$M = \frac{1}{2}\rho A h C_{\mathrm{M}} V_{\mathrm{rel}}^2 \tag{9}$$

where C_{M} is the corresponding aerodynamic coefficient. According to the quasi-steady methodologies, the aerodynamic moment is evaluated through Equation (9), and the limiting (accident) wind speed can be calculated, simply through a static equilibrium calculation, and some 'failure' criterion, such as a certain percentage of wheel unloading. All the quasi-steady methodologies developed over the years follow this general approach but differ in the definition of the aerodynamic coefficient. Some approaches have adopted coefficients based on

mean values of forces and velocities, while some have adopted coefficients based on extreme values of forces and velocities. The latter method is quite complex and the most simple way is to assume that the mean aerodynamic coefficient $\overline{C}_M$ is adequate for the evaluation of the extreme values of the aerodynamic forces and moments. This approach is adopted, for instance, in Japan [81,82], where a large experimental campaign has been carried out in order to account for the scenario effects (embankments of different heights and slopes, viaducts, bridges) in the evaluation of the mean aerodynamic coefficients. The critical wind velocities of overturning are then calculated through a static balance equation where, in addition to the aerodynamic moment and the centrifugal force, the inertia force induced by track irregularities is also accounted for.

In Germany, the new cross-wind guideline [83] has been in place from April 2006. According to this standard, the Characteristic Wind Curves (CWCs), defined as the limit wind speed that leads the vehicle to the overcoming of 90% wheel unloading, can be evaluated through both a simplified conservative approach based on a quasi-static vehicle dynamics [9] or the TSI time-domain method [84], described in the following.

In the first method, the stationary aerodynamic roll moment is calculated according to Equation (9), where $C_M = \overline{C}_M$ is the mean aerodynamic coefficient evaluated through low turbulence aerodynamic wind tunnel tests; the vehicle model is a five mass system with eleven degrees of freedom. The masses represent the carbody and the sprung and unsprung masses of the front and rear bogie. The masses are connected by force elements representing the primary and secondary stiffness and damping, an anti-roll bar and bump stops.

Since 2001, in the UK, the current approach to assess the stability of trains in high cross-winds is that reported in the Railway Safety Approved Code of Practice GC/RC5521 [38]: according to this standard, as aerodynamic coefficient, it has been adopted the '3 s' maximum coefficient experimentally evaluated through wind tunnel tests with boundary layer simulation in different operating conditions [11]. The overturning wind speed is computed using the aerodynamic rolling moment coefficient and the relative wind direction. The overturning wind speed and the gust wind speed (3-s average corresponding to a 1 in 50 year return period) are then combined to obtain the probability of occurrence of the critical gust during the passage of a train. An analysis of the uncertainties and bias associated to this methodology is reported in [11], where more refined approaches are introduced to account for the vehicle dynamical amplification.

7.2. *Time domain methods*

The most complex methodologies to model the wind–vehicle interaction have been developed in the time domain. Many researchers, in different countries, have developed different procedures to the evaluation of the wind safety limits of rail vehicles in cross-wind: the standard TSI approach set up within the European DEUFRAKO project between France and Germany [84,98]; the stochastic method, developed with different peculiarities in Italy [12,85], in the UK [86,77], in China [87]. Nevertheless, all these methodologies can be briefly described through the simple flow chart shown in Figure 28. The first step is about the definition of the wind speed field; the corresponding aerodynamic loads acting on the vehicle are then evaluated and represent the input of the multi-body dynamic simulation. Finally, the outputs are processed in order to evaluate the safety index and then to assess the limit wind speeds that lead the vehicle to the overcoming of the safety limit (CWC).

In the following Sections, the differences between methodologies in the definition/evaluation of the four steps of the common flow chart are described and the main peculiarities of each approach are highlighted.

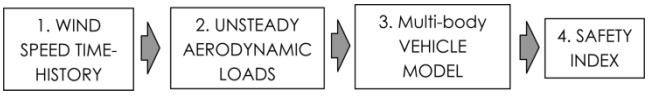

Figure 28. Common flow chart of the time-domain methods.

7.2.1. *Wind speed time-history*

Two main approaches can be followed to define the wind speed time-history:

(1) Equivalent gust representation: the turbulent wind is modelled through an ideal wind profile whose characteristics are considered as the most significant for the problem under study;
(2) Stochastic wind velocity field reconstruction: a realistic representation of the turbulent wind is made known its stochastic properties (turbulence intensity, integral length scale, PSD and coherence function).

In the railway field, the first approach has been followed by most railway operators in Europe during recent years: SNCF defined a bi-dimensional space 'rugby-ball' model to be combined with pressure distribution over the vehicle (experimentally measured through wind tunnel tests) in order to characterise the impact between the train and the wind gust, accounting for also the space distribution of the wind over the vehicle surface [88]. DB adopted a linear time model that starts from the mean wind speed and linearly increases up to the gust value and then remains constant. In Sweden, for the new high-speed Botniabanan line, a uniform constant wind profile has been considered but, in order to account for the interaction between actual wind gust duration (not infinite) and vehicle dynamics, especially when the vehicle exit from a tunnel, the calculated CWCs are then reduced by 5 m/s [19].

Most recently however, SNCF and DB have developed, within the DEUFRAKO Cross Wind project, a common methodology for the analysis of the cross-wind safety of high-speed railway operation [84]. The TSI standard provides a procedure based on a gust time–space model (bi-exponential) investigated in DEUFRAKO and named Chinese hat (Figure 29): this equivalent gust model approximates a random process in the vicinity of a local maximum and

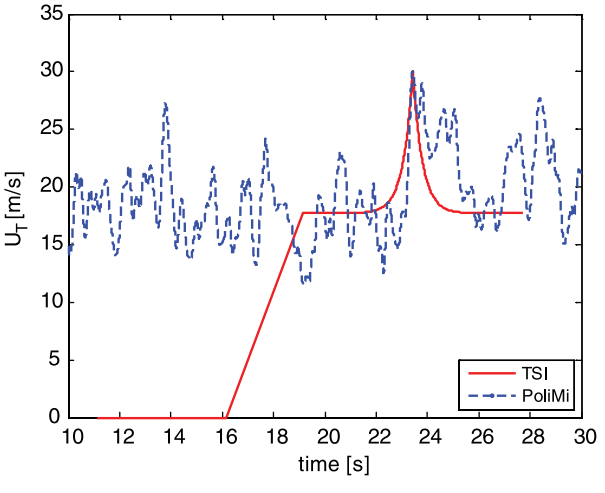

Figure 29. Wind speed time-history: Chinese hat equivalent gust profile (solid line) and stochastic wind (dashed line).

it corresponds to a fixed amplitude (equivalent to a probability level of amplitude ∼99%) and a probability level of exceedance of 50% for the gust duration (the mode of the distribution). The wind gust is evaluated for a fixed reference wind scenario, defined by the reference height ($z = 4$ m), the normalised gust amplitude and the roughness length of sites ($z_0 = 0.07$ m). Figure 29 shows an example of wind speed time-history generated according to the TSI specification. In the first section, the wind speed increases linearly from 0 to the mean wind speed; in the second section, the wind speed remains constant; the third section corresponds to the wind gust and, finally, the wind speed goes back to the mean value in the last section.

The second approach, to define the wind speed time history, is based on the reconstruction of the wind speed field where the vehicle is moving. Since turbulent wind is a stationary random process, starting from the statistical properties of the turbulent wind in the considered site, it is possible to evaluate a time–space distribution of the wind speed $U(t, x, y, z)$ (also shown in Figure 29). As known well, the simulation methods to define turbulent wind can be divided in two classes: WS (wave superposition methods) and ARMA (autoregressive-moving average modeling methods) [89].

The stochastic methodology [24,34] – developed by researchers of Politecnico di Milano, and actually adopted by Italian railway operators for the risk analysis of the new high-speed lines (Rome-Naples, Milano-Bologna, etc.) – adopts a modified WS method for the definition of the turbulent wind speed. Wind speed data are generated as a function of time and space $U(t, x, y, z)$: in the case of a moving train, taking into account the train trajectory and train velocity V_{tr}, it is possible to calculate the absolute wind speed $U_{\mathrm{T}}(t)$, in correspondence of a reference point moving with the vehicle itself. It is clear that, since the wind is a stochastic process, following the previously described procedure, it is possible to build up infinite time–space distributions of the absolute wind speed, all characterised by the same statistical properties and, as a consequence, the simulations of vehicles subjected to cross-wind have to be performed many times in order to allow a stochastic treatment of the results in terms of CWC.

A similar procedure has been recently adopted by Baker and his co-workers for the definition of a method for the integration of turbulent cross-wind forces into train dynamic calculations [77], ensuring that the wind speed time-history has the correct statistical and spectral properties. In [90] he uses a somewhat different approach, simulating the wind conditions only at the vehicle position at any one time. Also a method mentioned in [87] describes a framework for simulating railway vehicle and track interaction in cross-wind adopted for some applications in China; the wind speed time-histories are calculated through the WS method. In this procedure, in agreement with the approach adopted for bridges, both the longitudinal fluctuating component and the vertical fluctuating component of wind speed are simulated at a series of points along the vehicle way starting from the two-side cross-spectral density matrix of each component and by applying the Cholesky decomposition.

The stochastic approach allows to correctly reproduce the interaction between vehicle dynamics and turbulent wind, along space and time. While the equivalent gust method reproduces only one equivalent input, the stochastic approach, on the other hand, is more costly and time-consuming.

7.2.2. *Unsteady aerodynamic loads*

Once the wind speed time-history is known, the aerodynamic loads for a moving vehicle can be calculated according to two procedures:

- stationary approach;
- corrected quasi-steady approach.

The stationary approach consists of applying, instant by instant, the Equation (10), valid for stationary case:

$$F(t) = \frac{1}{2}\rho A C_{\mathrm{F}}(\beta(t)) V_{\mathrm{rel}}^2(t) \tag{10}$$

where $\beta = \beta(t)$ is the relative angle of attack time-history and the wind–train relative speed $V_{\mathrm{rel}}(t)$ is defined as

$$V_{\mathrm{rel}}^2(t) = (V_{\mathrm{tr}} + U_{\mathrm{T}}(t)\cos\alpha)^2 + (U_{\mathrm{T}}(t)\sin\alpha)^2. \tag{11}$$

According to the stationary approach, the relative wind–train speed is evaluated directly as a function of the absolute wind speed time-history U_{T} seen by the train. This procedure has been applied, for instance, in Germany and in Sweden.

The corrected quasi-steady approach is based on the application of the quasi-steady theory corrected by the admittance function, in the frequency domain, or, in the time domain, by the weighing function [76,90]. The admittance function accounts for the lack of spatial correlation of wind pressures at any two points on the carbody surface and then it represents a scaling factor to be applied to the ideal situation of a vehicle enveloped by turbulent wind with full spatial correlation. Due to the fact that the pressure distribution depends on vehicle geometry and on the turbulent wind speed characteristics, the admittance function has to be defined for each vehicle and for each wind scenario. It can be experimentally evaluated through full scale or wind tunnel tests [76] or it can be calculated through a numerical model [14].

According to the corrected quasi-steady approach, the Equation (11) becomes

$$V_{\mathrm{rel}}^2(t) = V_{\mathrm{rel\_TC}}^2(t) = (V_{\mathrm{tr}} + U_{\mathrm{TC}}(t)\cos\alpha)^2 + (U_{\mathrm{TC}}(t)\sin\alpha)^2 \tag{12}$$

where the quantity U_{TC} represents the corrected absolute wind speed in the reference point moving with the vehicle. This time-history can be computed using the admittance function or by calculating the convolution integral between the weighing function and the U_{T}. According to the TSI, the quantity U_{TC} is calculated in the time domain directly through a spatial-average filter, applied to the component U_{T}, with a window size equal to the vehicle length (but the filter is independent from the wind scenario).

7.2.3. *Multi-body model and safety index*

Multibody simulations are performed to determine the vehicle dynamic behaviour under a strong wind. The time-histories of the aerodynamic loads, evaluated according to the procedures previously presented, represent the input for the multi-body vehicle numerical model. In order to evaluate the CWC for each running condition, the numerical simulation results have been processed to calculate the limit safety conditions of the vehicle: the CWC represents the combination of train speed V_{tr} and limit wind speed U_{lim} which leads to the overcoming of a given safety limit.

For high-speed railway vehicles, the criterion most commonly adopted is the wheel unloading [9] defined as

$$\frac{\Delta Q}{Q_0} = 1 - \frac{Q_{i1} + Q_{j1}}{2 \cdot Q_0} < 0.9 \tag{13}$$

where Q_0 is the static vertical force on each wheel, Q_{ik} and Q_{jk} are the forces of the unloaded wheel belonging respectively to the first and second wheelset of the bogie.

Other criteria for the definition of the safety limit are the Prud'homme limit which limits the lateral track force and the Nadal criterion, which allows the evaluation of the safety to

derailment of a wheelset through placing a limit on the ratio of the lateral track force to the vertical force. These criteria are, in general, less critical at high speed, but they can become important under particular conditions through multibody simulations. It is therefore possible to define the wind velocity conditions leading to the overturning critical conditions shortly called CWC. An example of CWC is reported in Figure 30, where a comparison between a deterministic approach and a stochastic approach is reported. It is appreciable how the deterministic curve represents one of the possible solutions inside the spread of the stochastic approach result.

For road vehicles, the calculation methods for assessing vehicle performance in high cross-winds are very much less developed than for trains. This is probably due to the lack of a regulatory driver in the road vehicle industry that can impose the same constraints as the safety considerations that are the norm in the rail industry, but also because of the difficulties in adequately specifying driver behaviour. Some early work in determining road vehicle behaviour in cross-winds, including studies of course deflection and driver behaviour has been reported in the works of Baker [91,92]. The vehicle model used was, however, very simplistic and no proper allowance for suspension effects was included. More recently a number of multi-body simulations of road vehicles have been developed [93], which have much more realistic simulations of suspension effects, but still do not fully represent driver behaviour.

Figure 31 reports the results of the simulation of the dynamic response of a lorry during a U-turn movement under cross-wind effects. In the figure, the time-histories of the wind velocity (a), of the vertical loads (b) and of the safety index (c) are presented. As expected, the maximum load transfer occurs at curve entrance (after about 10 s of the simulation); after that, the load transfers both on the front and the rear axles decrease due to the fact that the wind mean direction is constant coming from the right side of the vehicle while the vehicle is turning; thus, changing the relative angle of attack between the vehicle and the mean wind speed.

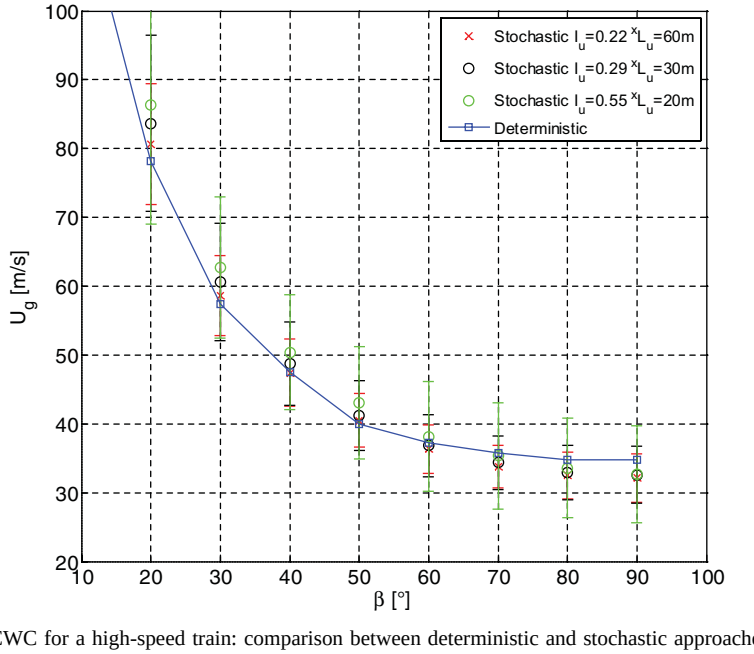

Figure 30. CWC for a high-speed train: comparison between deterministic and stochastic approaches (y axis is gust wind speed that causes overturning and β is the wind angle relative to the track).

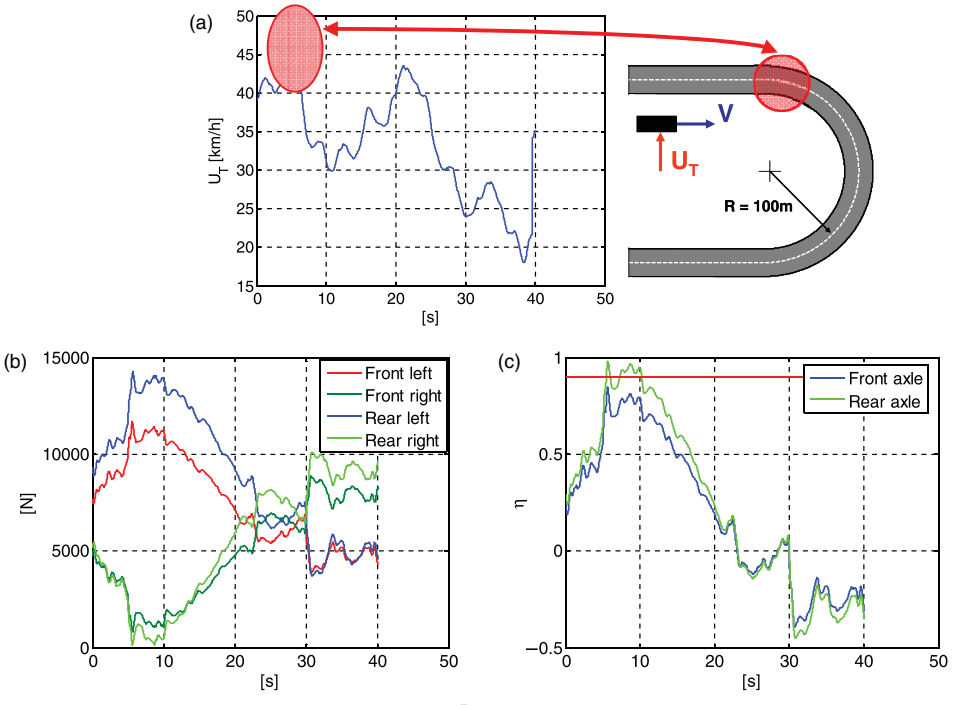

Figure 31. Lorry U-Turn simulation: $V = 45\,\text{km/h}$, $\bar{U} = 35\,\text{km/h}$, $R = 100\,\text{m}$, Iu = 30%, flat terrain. (a) Wind velocity time history (input of the model), (b) Wheel vertical loads time history (output of the model), (c) Time history of η index.

8. Risk-reduction techniques

Improvements of the cross-wind stability for a vehicle encompass a better aerodynamic design and an increase in the restoring moment. A reduction of the vehicle height and length would lead to a reduction of the aerodynamic roll moment and side force, but is in general not feasible. Increasing the weight by ballast will increase the restoring moment on the cost of higher axle load and energy consumption. Keeping the centre of gravity as low as possible will be beneficial to cross-wind stability. The global sensitivity, computed with the Morris method, of the cross-wind stability to various design parameters is exemplified in Figure 32. It can be seen that reduction of the aerodynamic roll moment and weight management are most influential to cross-wind stability and dominate measures on other parameters.

8.1. *Structural measures*

Porous or solid fences are passive infrastructure measures for the protection of wind-exposed sites at railway lines. Although aerodynamic forces on the fences itself have been studied intensively (see Section 6), much less is known for the influence of fences on the aerodynamic forces and moments that act on the vehicle. The influence of wind fences with various degrees of porosity on the aerodynamic side force has been reported in [82]. Recently, a detailed experimental study on the importance of height and inclination of fences has been carried out [94]. On the basis of these results, Figure 33 displays the influence of wind fences of different height (parameter η) on the critical wind speed. It indicates that with sufficiently

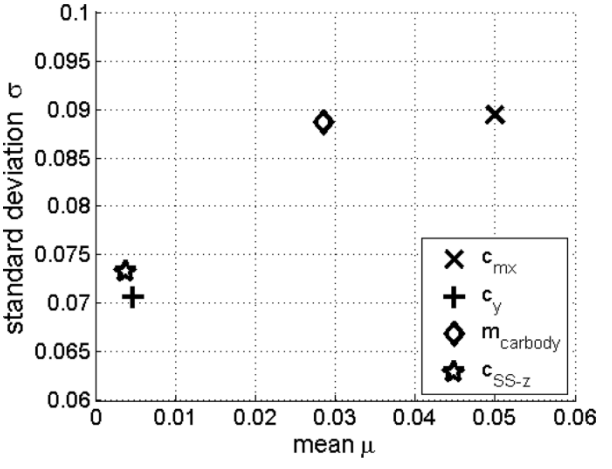

Figure 32. Global sensitivity analysis (Morris method) for aerodynamic and vehicle parameters.

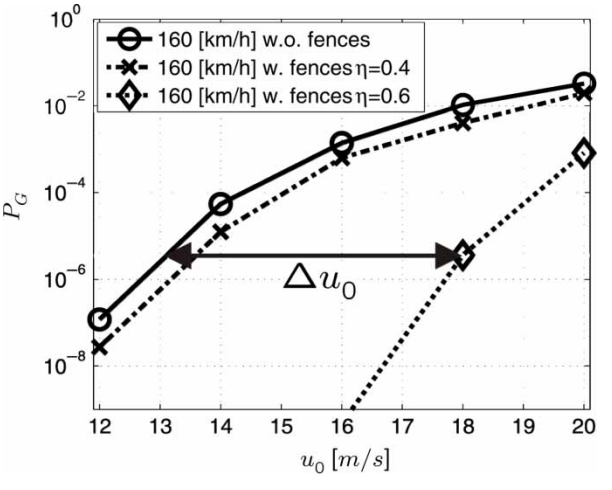

Figure 33. Influence of wind fences on the overturning probability (η indicates fence porosity).

high wind fences, a 30–40% larger wind velocity can be tolerated at the same risk. Full-scale tests showing the influence of fences on the roll moment are given in [42].

For the influence of the height and slope of embankments, the situation is more or less the same. Aerodynamic side force coefficients for trains on bridges of various heights and embankments of various heights and slopes are evaluated in [81,95]. Diedrichs *et al.* [96] report on a reduction of approximately 20% for the critical cross-wind velocity due to an embankment of 6-m height. Again, full-scale measurements demonstrating the influence of an embankment on the roll moment are given in [42].

Except for full-scale measurements, the use of a fixed train model in wind tunnel experiments does not reproduce the real situation, and absolute cross-wind stability predictions should be carefully interpreted. However, in order to judge the efficiency of structural measures, fixed train models seem to be sufficient.

8.2. *Technical measures*

In addition to structural safety measures, wind warning systems that issue velocity reductions or operation restrictions have been developed in France, Germany and Japan [27,82,97,99]. In France, a wind-monitoring system has been implemented in 2001 for the TGV-Mediterranée between Valence/Marseille and Avignon/Nîmes. In Japan, wind-warning systems have been established in 2005 on six exposed bridges of the major lines that link the Tokyo metropolitan area with its suburbs. In China, a system of meteorological sensors has been applied at strategic locations for the airport railway linking Lantau island with the city of Hong Kong. In Germany, a wind warning system has been developed and tested on the high-speed line between Berlin and Wolfsburg. European development activities on wind alarm systems for railway and road vehicle transport were concentrated in the project WEATHER within the sixth research framework programme of the European Union.

The Japanese wind-warning system works directly with the instantaneous wind velocity data from the anemometer and extrapolates by means of a Kalman filter an extreme wind velocity that corresponds to a given exceedance probability within the amount of time in which the train passes the bridge. If this extreme wind velocity is larger than a critical value, operational restrictions are issued. In [82], the wind-warning system has been extended by taking the wind direction into account and allowing for a dependence of operational measures on the expected wind direction.

The German wind-warning system 'Nowcasting' linearly extrapolates the 10-min averages of the wind velocity and the standard deviations for 2 min. The expected maximum wind velocity is then the sum of the extrapolated value, an extrapolation error and a gust supplement, which is obtained from the multiplication of the standard deviation for the wind velocity by a calibration factor. This calibration factor depends strongly on the extrapolated 10-min average wind velocity. The wind direction has been neglected in the model due to topographical conditions.

In France, a zonal observation system encompassing twelve sections of the TGV-Mediterranée line has been established. Each zone is assigned a wind measurement site that collects 10-min averages of the wind velocity and direction. The wind rose is divided into 36 sections of 10° degrees and for each of these sections; a critical wind velocity is computed by a risk-assessment procedure. The 10-min average values are extrapolated by means of a second-order auto-regressive model and operational restrictions enforced if the extrapolated wind velocity exceeds the critical value for the predicted wind direction. The critical wind velocities are determined by means of direct MCS from a prescribed failure probability conditioned on the wind velocity and direction at the wind measurement site. To this end, the measured average values at the site are transferred by normally distributed factors to instantaneous values at sections of 50-m length of the track. The instantaneous values of the wind velocity and direction are then compared with the CWC for the configuration (train speed, embankment height, cant, and so on) at this section and a failure event is generated if the value of the characteristic wind curve is exceeded. In order to adjust the level for the prescribed conditional failure probability, a risk-assessment procedure based on the distribution of the wind velocity and direction at the wind measurement site has to be carried out.

9. Conclusions and suggestions for further work

The knowledge of the cross-wind effects on vehicles, that initially was independently developed by different research groups, has nowadays reached some shared approach even if a completely standardised methodology is not yet assessed especially in the definition of the

risk analysis. The aim of improving vehicle interoperability, especially in the train field, and the development of high-speed train lines are pushing for the definition of national and European standards ruling the matter (even if the problem seems to be more frequent in the road vehicles).

Experimental techniques to define aerodynamic coefficients have reached some common practical rules as the adoption of a common scenario for wind tunnel tests on still models. The ongoing research is now investigating on moving vehicles test rigs to analyse the effects of the relative velocity between the vehicle and the infrastructure scenarios.

CFD numerical techniques are becoming more affordable and show interesting results in comparison with experimental results at low yaw angles while more sophisticated and demanding models are required for large angle of attack where large flow separation occurs.

Multi-body numerical techniques represent the more reliable approach to take into account the dynamic interaction between the response of the vehicle and the wind loads. Some uncertainties (mechanical parameters, contact modelling, driver control laws, and so on) are also present in the multi-body modelling and have to be taken into account in the overall risk analysis especially for road vehicles, where the driver behaviour is important in the definition of the vehicle's response.

The definition of the overturning risk assessment represents a very complicated matter due to the large number of random variables playing roles in the cross-wind aspects. Affordable computational procedures for the failure probability rely on reduction of the model complexity through sensitivity analysis and variance reduction in the simulations.

The literature presents several attempts to consider the variability of different parameters (meteo, wind-vehicle interaction, line description, and so on) in order to define which are the most important in the cross-wind risk analysis, and different approaches are proposed to face the problem even if a common agreement is not yet reached.

In the meanwhile, some solutions to reduce the risk of vehicle overturning due to cross-wind effects are yet adopted as real-time meteo alert systems. Similar systems are based on risk analysis of real railway lines or motorways and represent an alternative approach to wind shields.

There are however still major challenges for the future. While wind tunnel and full-scale experimental techniques are well established as tools for the determination of aerodynamic force and moment coefficients, the use of CFD techniques still requires further development and calibration against experimental values before it can be used in routine calculations for new vehicles. There are also a number of classes of vehicles that are potentially at risk during cross-winds that have not yet been fully investigated – for example, different geometries of high-sided road vehicle and articulated trains. Also the relative merits of the different types of risk-assessment techniques need to be evaluated and which method is the best to be used in specific situations needs to be clarified.

References

[1] C.J. Baker and S. Reynolds, *Wind induced accidents of road vehicles*, Accid. Anal. Prev. 24(6) (1991), pp. 559–575.
[2] C.J. Baker, *A simplified analysis of various types of wind induced road vehicle accidents*, J. Wind Eng. Ind. Aerodyn. 22(1) (1986), pp. 69–85.
[3] C.J. Baker, *The overturning of road and rail vehicles in high winds*, Proceedings of Asia Pacific Regional Conference on Wind Engineering, Seoul, Korea, 2005.
[4] Xinhua News Agency, *Train overturned by strong wind in NW China*, February 28, 2007. Available at http://www.highbeam.com/doc/1P2-16122353.html
[5] http://www.redorbit.com/news/general/340348/japan_train_derailment_leaves_four_dead/, accessed 11 April 2009.

[6] E. Andersson, J. Häggström, M. Sima, and S. Stichel, *Assessment of train-overrturning risk due to strong cross-winds*. Proc. IMechE F: J. Rail Rapid Transit 218 (2004), pp. 213–223.
[7] CEN. prEN 14067 – *Railway applications aerodynamics Part 6: Requirements and test procedures for cross wind assessment*, European Norm, CEN/TC 256, 2008.
[8] EC. TSI Commission Decision of 21 February 2008 concerning a technical specification for interoperability relating to the 'rolling stock' sub-system of the trans-European high-speed rail system, section 4.2.6.3. Crosswind, Official Journal of the European Union, pp. 193–195, 2008.
[9] Th. Tielkes, Ch. Heine, M. Möller, and J. Driller, *A probabilistic approach to safeguard cross wind safety of passenger railway operation in Germany: The new DB guideline Ril 80704*, Proceedings of the 8th World Congress on Railway Research, Seoul, South Korea, 2008.
[10] P.-E. Gautier, Ch. Sacre, D. Delaunay, M. Parrot, Ch. Dersigny, and S. Bodere, *TGV Méditerranée high speed line safety against cross-winds: a slow-down system based on anemometric measurements and spatial short-term meteorological prediction*, Proceedings of the 5th World Congress on Railway Research, Köln, Germany, 2001.
[11] W.M.S. Bradbury, P. Pottrill, and V. Murtagh, *Enhanced permissible speed on the West Coast mainline: Investigations of wind overturning effects*, Proceedings of the 6th World Congress on Railway Research, Edinburgh, UK, 2003, pp. 476–485.
[12] F. Cheli, R. Corradi, G. Diana, and G. Tomasini, *A numerical-experimental approach to evaluate the aerodynamic effects on rail vehicle dynamics*, Vehicle Syst. Dyn. Suppl. 41 (2004), pp. 707–716.
[13] A. Bouferrouk, C.J. Baker, M. Sterling, H. O'Neil, and S. Wood, (2008) *Calculation of the cross wind displacement of pantographs*, Colloquium on Bluff Body Aerodynamics and its Applications, Milano, Italy.
[14] R.K. Cooper, *The probability of trains overturning in high winds*, Proceedings of 5th International Conference on Wind Engineering, Fort Collins, Colorado, July 1979.
[15] H.J. Roodbaraky, C.J. Baker, A.R. Dawson, and C.J. Wright, *Experimental observations of the aerodynamic characteristics of urban trees*, J. Wind Eng. Ind. Aerodyn. 52 (1994), pp. 171–184.
[16] A.D. Quinn, C.J. Baker, and N.G. Wright, *Wind and vehicle induced forces on flat plates, Part 1: Wind induced force*, J. Wind Eng. Ind. Aerodyn. 89 (2001), pp. 817–829.
[17] C. Baker, M. Sterling, T. Johnson, G. Figura-Hardy, and C. Pope, *The effect of crosswinds on train slipstreams*, International Conference on Wind Engineering, Cairns, Australia, 2007.
[18] R.P. Hoxey, P.J. Kettlewell, A.M. Meehan, C.J. Baker, and X. Yang, *The aerodynamics and ventilation of poultry transport vehicles, Part 1: Full scale experiments*, J. Agric. Eng. Res. 65 (1996), pp. 77–83.
[19] CENELEC Standard EN 50126: *Railway applications – The specification and demonstration of dependability, reliability, maintainability and safety (RAMS)*, 2000.
[20] Edwards vs. The National Coal Board: [1949] 1 All ER 743 (CA).
[21] DB AG, *Handbuch für den Sicherheitsnachweis bei Seitenwind*, München, 2001.
[22] T. Payer and H. Küchenhoff.: *Modelling extreme wind speeds at a German weather station as basic input for a subsequent risk analysis for high-speed trains*, Wind Eng. Ind. Aerodyn. 92 (2004), pp. 241–261.
[23] A. Carrarini, *Reliability based analysis of the crosswind stability of railway vehicles*, Wind Eng. Ind. Aerodyn. 95 (2007), pp. 493–509.
[24] G. Diana, M. Burlando, F. Cheli, A. Freda, C.F. Ratto, D. Rocchi, G. Solari, M. Testa, and G. Tomasini, *A new methodology to perform the risk analysis of cross wind on high speed lines*, 8th World Congress on Railway Research (WCRR 2008), Seoul, Korea, 18–22 May 2008.
[25] R.D. Reiss and M. Thomas, *Statistical Analysis of Extreme Values*, Birkhäuser, Basel, 2007.
[26] P.L. Liu and A. Der Kiureghian, *Optimization algorithms for structural reliability*, Struct. Safety 9 (1991), pp. 161–177.
[27] M. Shimamura and N. Kobayashi, *Development of a strong wind warning system*, Jpn. Railway Eng. 150 (2003), pp. 13–15.
[28] A. Nataf, *Détermination des distributions de probabilités dont les marges sont données*, C. R. Acad. Sci. 225 (1962), pp. 42–43.
[29] M. Rosenblatt, *Remarks on a multivariate transformation*, Ann. Math. Stat. 23(3) (1952), pp. 470–72.
[30] K. Breitung, *Asymptotic approximations for multinormal integrals*, J. Eng. Mech. (ASCE) 110(3) (1984), pp. 357–367.
[31] H.J. Pradlwarter, G.I. Schueller, P.S. Koutsourelakis, and D.C. Charmpis, *Application of line sampling simulation method to reliability benchmark problems*, Struct. Safety 29 (2007), pp. 208–221.
[32] H. Liu, W. Chen, and A. Sudjianto, *Probabilistic sensitivity analysis methods for design under uncertainty*, Proceedings of 10th AIAA/ISSMO Multidisciplinary Analysis and Optimization Conference, Albany, New York, 2004.
[33] M.D. Morris, *Factorial sampling plans for preliminary computational experiments*, Technometrics 33 (1991), pp. 161–174.
[34] F. Cheli, R. Corradi, D. Rocchi, G. Tomasini, and E. Maestrini, *Wind tunnel tests on train scale models to investigate the effect of infrastructure scenario*, VI International Colloquium on Bluff Bodies Aerodynamics & Applications (BBAA VI), Milano, Italy, July 20–24, 2008.
[35] M. Schober, M. Weise, A. Orellano, P. Deeg, and W. Wetzel, *Wind tunnel investigation of an ICE 3 on an embankment*, VI International Colloquium on Bluff Bodies Aerodynamics & Applications (BBAA VI), Milano, Italy, July 20–24, 2008.

[36] N. Rüd and T. Tielkes. *Reference wind tunnel measurements on aerodynamic coefficients of ICE3 end car*, Proceedings of the EuroMech Colloquium 509 on Vehicle Aerodynamics, Berlin, Germany, 2009, p. 39.
[37] D. Rocchi, M. Schober, A. Orellano, F. Cheli, and G. Tomasini, *Comparison of wind tunnel tests results on the ATM train*, Proceedings of the EuroMech Colloquium 509 on Vehicle Aerodynamics, Berlin, Germany, 2009, p. 39.
[38] GC/RC5521, Issue 1 Railway Safety Approved Code of Practice "Calculation of Enhanced Permissible Speeds for Tilting Trains" of June 2001
[39] M. Bocciolone, F. Cheli, R. Corradi, S. Muggiasca, and G. Tomasini, *Crosswind action on rail vehicles: wind tunnel experimental analyses*, J. Wind Eng. Ind. Aerodyn. 96 (2008), pp. 584–610.
[40] C.J. Baker, *Train aerodynamic forces and moments from moving model experiments*, J. Wind Eng. Ind. Aerodyn. 24(3) (1986), pp. 227–252.
[41] M. Sterling, A.D. Quinn, D.M. Hargreves, F. Cheli, E. Sabbioni, G. Tomasini, D. Delaunay, C.J. Baker, and H. Morvan, *A comparison of different methods to evaluate the wind induced forces on a high sided lorry*, J. Wind Eng. Ind. Aerodyn., submitted for publication
[42] G. Matschke and C. Heine, *Full scale tests on side wind effects on trains. Evaluation of aerodynamic coefficients and efficiency of wind breaking devices*, in *TRANSAERO: A European Initiative of Transient Aerodynamics for Railway System Optimisation*, B. Schulte-Werning, R. Grégoire, A. Malfati, and G. Matschke, eds., Springer, Berlin, 2002, pp. 27–38.
[43] C.J. Baker, F. Lopez-Calleja, J. Jones, and J. Munday, *Measurements of the cross wind forces on trains*, J. Wind Eng. Ind. Aerodyn. 92 (2004), pp. 547–563.
[44] K. Tanemoto, M. Suzuki, H. Saito, and T. Imai, Wind tunnel tests on aerodynamic characteristics of train/vehicles in cross winds and effects of wind-protection fences, RTRI Rep. 18(9) (2004), pp. 17–22.
[45] B. Diedrichs, *Unsteady aerodynamic crosswind stablity of a high-speed train subjected to gusts of various rates*, Proceedings of the EuroMech Colloquium 509 on Vehicle Aerodynamics, Berlin, Germany, 2009, p. 39.
[46] S. Krajnovic, *Shape optimization of a bus for crosswind stability*, Proceedings of the EuroMech Colloquium 509 on Vehicle Aerodynamics, Berlin, Germany, 2009, p. 39.
[47] E. Guilmineau and F. Chometon, *Experimental and numerical study of unsteady wakes behind an oscillating car model*, Proceedings IUTAM Symposium, Corfu, 2007.
[48] P.-A. Mackrodt and E. Pfizenmaier, Aerodynamik und Aeroakustik für Hochgeschwindigkeitszüge. Phys. Unserer Zeit 18 (1987), pp. 65–76.
[49] T.W. Chiu, *Prediction of the aerodynamic loads on a railway train in a cross-wind at large yaw angles using an integrated two- and three-dimensional source/vortex panel method*, J. Wind Eng. Ind. Aerodyn. 57(1) (1995), pp. 19–39.
[50] S.V. Pantakar and D.B. Spalding, *A calculation procedure for heat, mass and momentum transfer in parabolic flow*, Int. J. Heat Mass Tranfer 15 (1972), pp. 1787–1806.
[51] N.G. Markatos, *The theoretical prediction of external aerodynamics of road vehicles*, Int. J. Vehicle Des. SP3 (1983), pp. 387–400.
[52] F. Menter, *Two-equation eddy-viscosity turbulence model for engineering applications*, AIAA J. 32 (1994), pp. 1598–1605.
[53] K. Hanjalic and S. Jakirlic, *Second-moment turbulence closure modeling*, in *Closure Strategies for Turbulent and Transitional Flows*, B.E. Launder and N. Sandham, eds., Cambridge University Press, Cambridge, UK, 2002, pp. 47–101.
[54] W. Khier, M. Breuer, and F. Durst, *Numerical computation of 3D turbulent flow around high speed train under side wind conditions*, in *TRANSAERO: A European Initiative of Transient Aerodynamics for Railway System Optimisation*, B. Schulte-Werning, R. Grégoire, A. Malfati, and G. Matschke, eds., Springer, Berlin, 2002, pp. 75–84.
[55] D. Wu, *Predictive prospects of unsteady detached-Eddy simulations in industrial external aerodynamic flow simulations*, Diploma thesis, Lehrstuhl fur Strömungslehre und Aerodynamik, Aachen, Germany, 2004.
[56] H. Hemida and S. Krajnović, *Numerical study of the unsteady flow structures around train-shaped body subjected to side winds*, European Conference on Computational Fluid Dynamics, Delft, The Netherlands, 2006.
[57] B Diedrichs, *Computational methods for crosswind stability of railway trains – a literature survey*, KTH Engineering Sciences Report TRITA AVE 2005:27, 2005.
[58] A. Ryan and R.G. Dominy, *Wake survey behind a passenger car subjected to a transient cross-wind gust*, SAE 2000-01-0874, 2000.
[59] M. Juhlin and P. Eriksson, A *vehicle parameter study on crosswind sensitivity of buses*, SAE Technical Paper, 2004-01-261, 2004.
[60] D.K. Lilly, *The representation of small-scale turbulence in numerical simulation experiments*, in H.H. Goldstein, ed., Proceedings of IBM Scientific Computing Symposium on Environmental Sciences, IBM Forum No. 320-1951, 1976, pp. 195–210.
[61] M. Germano, U. Piomelli, P. Moin, and W.H. Cabitt, Dynamic subgrid-scale Eddy viscosity model, Phys. Fluids A 3(7) (1991), pp. 1760–1765.
[62] C. Rolén, T. Rung, and D. Wu, *Computational modelling of cross-wind stability of high speed trains*, in *European Congress on Computational Methods in Applied Sciences and Engineering*, P. Neittaanmäki, T. Rossi, S. Korotov, E. Oñate, J. Périaux, and D. Knörzer, eds., Eccomas, 2004, pp. 1–20.

[63] U. Frisch, B. Hasslacher, and Y. Pomeau, *Lattice-Gas automata for the Navier–Stokes equation*, Phys. Rev. Letter 56(14) (1986), pp. 1505–1508.
[64] M. Krafcyck, Gitter *Boltzmann Methoden: Von der Theorie zur Anwendung*, Habilitation thesis, Technische Universität München, 2001.
[65] W.A. Mair and A.J. Stewart, *The flow past yawed slender bodies, with and without ground effects*, J. Wind Eng. Ind. Aerodyn. 18 (1985), p. 301.
[66] J.M. Copley, *The 3-D flow around railway trains*, J. Wind Eng. Ind. Aerodyn. 26, pp. 21, 1987.
[67] C.G. Robinson and C.J. Baker, *The effect of atmospheric turbulence on trains*, J. Wind Eng. Ind. Aerodyn. 34 (1990), pp. 251–272.
[68] R. Klein and J. Hogue, *Effects of crosswinds on vehicle response – Full-scale tests and analytical predictions*, SAE paper 800848, 1980.
[69] H.N. Hemida, *Large Eddy simulation of the flow around simplified high speed trains under side wind conditions*, Licentiate of Engineering thesis, Chalmers University of Technology, Goteborg, Sweden, 2006.
[70] S.A. Coleman and C.J. Baker, *An experimental study of the aerodynamic behaviour of high sided lorries in cross winds*, J. Wind Eng. Ind. Aerodyn. 53(3) (1994), pp. 401–431.
[71] M. Juhlin, *Assessment of crosswind performance of buses*, PhD-thesis in Vehicle Engineering, ISSN 1651-7660, KTH, Sweden, 2009.
[72] J. Petzäll, P.Å. Torlund, T. Falkmer, P. Albertsson, and U. Björnstig, *Aerodynamic design of high-sided coaches to reduce cross-wind sensitivity, based on wind tunnel tests*, Int. J. Crashworthiness 13(2) (2008), pp. 185–194.
[73] M.J. Stewart, *Transient aerodynamic forces on simple road vehicle shapes in simulated cross-wind gusts*, MIRA research report No. 1977/5, 1977.
[74] I. Kohri and T. Kataoka, *Research on improvement of cross-wind properties of passenger vehicles*, JSAE Rev. 10(3) (1989), pp. 46–51.
[75] B. Diedrichs, *Aerodynamic calculations of crosswind stability of a high-speed train using control volumes of arbitrary polyhedral shape*, BBAA VI 2008.
[76] M. Sterling, C.J. Baker, A. Bouferrouk, H. ONeil, S. Wood, and E. Crosbie, *An investigation of the aerodynamic admittances and aerodynamic weighting functions of trains*, J. Wind Eng. Ind. Aerodyn., submitted for publication
[77] Y. Ding, M. Sterling, and C.J. Baker, *An alternative approach to modelling train stability in high cross winds*, Proc. IMechE F: J. Rail Rapid Transit 222(1) (2008), pp. 85–97.
[78] C.J. Baker, *Ground vehicles in high cross winds, Part 1: Steady aerodynamic forces* J. Fluids Struct. 5 (1991), pp. 69–90.
[79] C.J. Baker, *Ground vehicles in high cross winds, Part 2: Unsteady aerodynamic forces*, J. Fluids Struct. 5 (1991), pp. 91–111.
[80] C.J. Baker, *Ground vehicles in high cross winds, Part 3: The interaction of aerodynamic forces and the vehicle system*, J. Fluids Struct. 5 (1991), pp. 221–241.
[81] T. Fujii, T. Maeda, H. Ishida, T. Imai, K. Tanemoto, and M. Suzuki, *Wind-induced accidents of trains/vehicles and their measures in Japan*, Q. Rep. RTRI 40(1) (1999), pp. 50–55.
[82] T. Imai, T. Fujii, K. Tanemoto, T. Shimamura, T. Maeda, H. Ishida, and Y. Hibino, *New train regulation method based on wind direction and velocity of natural wind against strong winds*, J. Wind Eng. Ind. Aerodyn. 90 (2002), pp. 1601–1610.
[83] DB Netz AG, *Richtlinie 807.04 Bautechnik, Leit-, Signal- und Telekommunikationstechnik. Ausgewählte Maßnahmen und Anforderungen and das Gesamtsystem Fahrweg/Fahrzeug –Aerodynamik/Seitenwind*, DB Netz AG, Frankfurt, 2006.
[84] P.-E. Gautier, Th. Tielkes, F. Sourget, E. Allain, M. Grab, and Ch. Heine, *Strong wind risks in railways: the DEUFRAKO crosswind program*, Proceedings of the 6th World Congress on Railway Research, Edinburgh, UK, 2003, pp. 463–475.
[85] R. Cheli, G. Mancini, R. Roberti, G. Diana, F. Cheli, R. Corradi, and G. Tomasini, *Cross-wind aerodynamic forces on rail vehicles: wind tunnel experimental tests and numerical dynamic analysis*, WCRR, Edinburgh, UK, 2003.
[86] C.J. Baker, A. Bouferrouk, J. Perez, and S.D. Iwnicki, *The integration of cross wind forces into train dynamic calculations*, Proceedings of the 8th World Congress on Railway Research, South Korea, 2008.
[87] Y.L. Xu and Q.S. Ding, (2006). *Interaction of railway vehicles with track in cross-winds*, J. Fluids Struct. 22(3), pp. 295–314.
[88] L.M. Cleon and A Jourdain, *Protection of line LN5 against cross winds*, Proceedings of the 5th World Congress on Railway Research, Köln, Germany, 2001.
[89] Y. Iwatani, *Simulation of multidimensional wind fluctuations having arbitrary power spectra and cross spectra*, J. Wind Eng. Ind. Aerodyn. 11 (1982), pp. 5–18.
[90] C.J. Baker, *The simulation of unsteady aerodynamic cross wind forces on trains*, J. Rail Rapid Transit, submitted for publication.
[91] C.J. Baker, *Measures to control vehicle movement at exposed sites during windy periods*, J. Wind Eng. Ind. Aerodyn. 25 (1987), pp. 151–167.
[92] C.J. Baker, *High sided articulated lorries in strong cross winds*, J. Wind Eng. Ind. Aerodyn. 31 (1988), pp. 67–85.

[93] D. Delaunay, C.J. Baker, F. Cheli, H. Morvan, L. Berger, M. Casazza, C. Gomez, C. Le Cleac'h, R. Saffell, R. Grégoire, and A. Viñuales, *Development of wind alarm systems for road and rail vehicles: presentation of the WEATHER project*, SIRWEC 2006: 13th Int. Road Weather Conference, 2006.
[94] M.A. Barcala and J. Meseguer, *An experimental study of the influence of parapets on the aerodynamic loads under cross wind on a two-dimensional model of a railway vehicle on a bridge*. Proc. IMechE F: J. Rail Rapid Transit 221 (2007), pp. 487–494.
[95] M. Suzuki, K. Tanemoto, and T. Maeda, *Aerodynamic characteristics of train/vehicles under cross winds*, Wind Eng. Ind. Aerodyn. 91 (2003), pp. 209–218.
[96] B. Diedrichs, M. Sima, A. Orellano, and H. Tengstrand, *Crosswind stability of a high-speed train on a high embankment*, Proc. IMechE F: J. Rail Rapid Transit 221(2) (2007), pp. 205–227.
[97] D. Delaunay, L.M. Cléon, C. Sacré, F. Sourget, and P.E. Gautier, *Designing a wind alarm system for the TGV-Méditerranée*, Proceedings of 11th International Conference on Wind Engineering, Lubbock, TX, USA, June 2003.
[98] L.-M. Cléon, P.-E. Gautier, and F. Sourget, *Sécurité de la circulation des trains à grande vitesse vis-à-vis des vents latéraux: le programme DeuFraKo*, Rev. Gen. Chemins Fer 2004 (7) (July 2004).
[99] U. Hoppmann, S. König, T. Tielkes, and G. Matschke, *A short-term wind prediction model for railway application: design and verification*, Wind Eng. Ind. Aerodyn. 90(10) (2002), pp. 1601–1610.